ORIGINAL PAPER

PP2A and GSK3 act as modifiers of FUS-ALS by modulating mitochondrial transport

Paraskevi Tziortzouda[1,2] · Jolien Steyaert[1,2] · Wendy Scheveneels[1,2] · Adria Sicart[1,2] · Katarina Stoklund Dittlau[1,2] · Adriana Margarida Barbosa Correia[1,2,3] · Thibaut Burg[1,2] · Arun Pal[4,5] · Andreas Hermann[5,6,7,8] · Philip Van Damme[1,2,9] · Thomas G. Moens[1,2] · Ludo Van Den Bosch[1,2]

Abstract

Amyotrophic lateral sclerosis (ALS) is a fatal neurodegenerative disease which currently lacks effective treatments. Mutations in the RNA-binding protein FUS are a common cause of familial ALS, accounting for around 4% of the cases. Understanding the mechanisms by which mutant FUS becomes toxic to neurons can provide insight into the pathogenesis of both familial and sporadic ALS. We have previously observed that overexpression of wild-type or ALS-mutant FUS in *Drosophila* motor neurons is toxic, which allowed us to screen for novel genetic modifiers of the disease. Using a genome-wide screening approach, we identified Protein Phosphatase 2A (PP2A) and Glycogen Synthase Kinase 3 (GSK3) as novel modifiers of FUS-ALS. Loss of function or pharmacological inhibition of either protein rescued FUS-associated lethality in *Drosophila*. Consistent with a conserved role in disease pathogenesis, pharmacological inhibition of both proteins rescued disease-relevant phenotypes, including mitochondrial trafficking defects and neuromuscular junction failure, in patient iPSC-derived spinal motor neurons (iPSC-sMNs). In FUS-ALS flies, mice, and human iPSC-sMNs, we observed reduced GSK3 inhibitory phosphorylation, suggesting that FUS dysfunction results in GSK3 hyperactivity. Furthermore, we found that PP2A acts upstream of GSK3, affecting its inhibitory phosphorylation. GSK3 has previously been linked to kinesin-1 hyperphosphorylation. We observed this in both flies and iPSC-sMNs, and we rescued this hyperphosphorylation by inhibiting GSK3 or PP2A. Moreover, increasing the level of kinesin-1 expression in our *Drosophila* model strongly rescued toxicity, confirming the relevance of kinesin-1 hyperphosphorylation. Our data provide in vivo evidence that PP2A and GSK3 are disease modifiers, and reveal an unexplored mechanistic link between PP2A, GSK3, and kinesin-1, that may be central to the pathogenesis of FUS-ALS and sporadic forms of the disease.

Keywords Amyotrophic lateral sclerosis · *Drosophila* · PP2A · GSK3 · Kinesin

✉ Thomas G. Moens
thomas.moens@kuleuven.be

✉ Ludo Van Den Bosch
ludo.vandenbosch@kuleuven.be

1   Department of Neurosciences, Experimental Neurology and Leuven Brain Institute (LBI), KU Leuven-University of Leuven, Leuven, Belgium

2   Center for Brain & Disease Research, Laboratory of Neurobiology, VIB, Campus Gasthuisberg, O&N5, Herestraat 49, PB 602, 3000, Leuven, Belgium

3   Instituto Superior Técnico-Universidade de Lisboa, Av. Rovisco Pais, 1049-001 Lisbon, Portugal

4   Dresden High Magnetic Field Laboratory (HLD-EMFL), Helmholtz-Zentrum Dresden Rossendorf, 01328 Dresden, Germany

5   Division of Neurodegenerative Diseases, Department of Neurology, Technische Universität Dresden, 01307 Dresden, Germany

6   Translational Neurodegeneration Section "Albrecht Kossel", Department of Neurology, University Medical Center Rostock, University of Rostock, 18147 Rostock, Germany

7   Deutsches Zentrum Fur Neurodegenerative Erkrankungen (DZNE) Rostock/Greifswald, 18147 Rostock, Germany

8   Center for Transdisciplinary Neurosciences Rostock (CTNR), University Medical Center Rostock, University of Rostock, 18147 Rostock, Germany

9   Department of Neurology, University Hospitals Leuven, Leuven, Belgium

Introduction

Amyotrophic lateral sclerosis (ALS) is the most common motor neuron disease in adults, characterized by selective loss of upper and lower motor neurons in the brain and spinal cord [28, 40]. Symptoms include muscle wasting and paralysis, and death usually occurs within an average of three years post-diagnosis due to failure of the respiratory muscles [28]. In 90% of cases, ALS is sporadic (sALS) with no known family history [40]. However, 10% of cases are familial (fALS), where patients inherit the disease mostly in an autosomal dominant manner [40]. Mutations in the *Fused in Sarcoma (FUS)* gene, encoding the FUS protein, account for ~4% of fALS and ~1% of sALS cases [40]. FUS is a DNA/RNA-binding protein, and in mutation carriers, it mislocalizes to the cytoplasm where it aggregates [40].

Despite advances in the understanding of the genetics and pathogenesis of ALS, effective therapeutic options are currently lacking, with licensed drugs extending the lifespan of patients by only a few months [28]. Here, we aimed to identify new targets involved in the pathogenesis of FUS-associated ALS using *Drosophila* and induced pluripotent stem cell-derived spinal motor neuron (iPSC-sMN) models.

As a human model of FUS-associated fALS, we previously generated and extensively characterized iPSC-sMNs from *FUS* mutation carriers as well as their isogenic controls [29, 61, 74]. In these sMNs, we observed FUS cytoplasmic mislocalization, similar to that reported in cellular models and patient *post-mortem* material [17]. In addition, we observed a mitochondrial neuritic transport defect [29], which we have since confirmed is a common phenotype in iPSC-sMNs from *TARDBP* and *C9orf72* familial-ALS mutation carriers [22, 24]. This suggests that mitochondrial transport defects could be a common underlying disease mechanism in ALS. Recently, we also demonstrated that the *FUS* mutant sMNs fail to correctly form neuromuscular junctions (NMJs) when cultured with human primary mesoangioblast-derived myotubes in microfluidic devices [61].

We previously showed that overexpression of wild-type or ALS-mutant FUS in *Drosophila* motor neurons is toxic, leading flies to die in their pupal cases. Therefore, this *Drosophila* model provides a useful screening tool to identify candidate modifying genes [5, 37]. Using eclosion as a readout, we performed a genome-wide genetic screen to identify modifiers of FUS-ALS in vivo, and found that *microtubule star* (*mts*) (the *Drosophila* ortholog of *PPP2CA*) and *shaggy* (*sgg*) (the *Drosophila* ortholog of *GSK3B*), are novel modifiers of FUS-associated ALS. Specifically, genetic and pharmacological inhibition of

mts and sgg rescued eclosion and lifespan of FUS flies. Importantly, PP2A and GSK3 pharmacological inhibition in human cells rescued hallmark ALS-associated phenotypes, including FUS cytoplasmic mislocalization, NMJ formation, and mitochondrial transport defects. Interestingly, GSK3 inhibitory phosphorylation appeared reduced in our FUS-ALS models, suggesting that FUS dysfunction results in GSK3 hyperactivity. We also found that the phosphatase PP2A acts upstream of GSK3, altering its inhibitory phosphorylation, in both flies and human cells.

Mitochondrial transport is a vital process mainly mediated by the motor protein kinesin [30, 57], and GSK3 has been shown to phosphorylate kinesin-1 in *Drosophila* and mammalian cells [2, 46]. Hence, GSK3 hyperactivity could cause kinesin hyperphosphorylation and dysfunction, explaining the mitochondrial transport deficits observed in patient sMNs. Excitingly, we observed that PP2A and GSK3 inhibition can rescue mitochondrial transport deficits in FUS-ALS patient iPSC-sMNs, and kinesin-1 appears as an intermediate regulator of this cascade. Altogether, by looking from fly to human, our data provide further insight into the mechanisms of FUS toxicity, and have identified PP2A and GSK3 as novel disease modifiers and potential therapeutic targets for ALS.

Materials and methods

Drosophila lines and maintenance

Drosophila melanogaster strains were maintained on standard medium (62.5 g/L cornmeal, 25 g/L yeast, 7 g/L agar, 16.9 g/L dextrose, 37.5 mL/L golden syrup, 9.375 mL/L propionic acid, 1.4 g/L hydroxybenzoate, and 14.0 mL/L ethanol) in a 12 h light/dark rhythm. The UAS-FUS lines have been described previously [5]. The following stocks were obtained from the Bloomington *Drosophila* Stock Center (BDSC): D42-Gal4 (8816), Gal80-ts (7019), nSyb-Gal4 (51635), sgg RNAi#1 (31308), sgg RNAi#2 (31309), sgg RNAi#3 (38293), sgg RNAi#4 (35364), *UAS-sgg WT* (5361), *UAS-sgg S9A* (5255), null mutant mts^{XE2258} (5684), and null mutant sgg (4095). The following lines were obtained from the Vienna *Drosophila* RNAi Center (VDRC): mts RNAi#1 (35171), mts RNAi#2 (35172), and mts RNAi#3 (41924). The Khc line *w;;p[Khc+]* was provided by William Saxton (University of California, Santa Cruz).

For backcrossing: The *w1118* (Canton-S10) line was used as a background control, and for experiments using TRiP lines, a stock consisting of *w + v- X* chromosome in the *w1118* genetic background (provided by Teresa Niccoli, University College London) was used. Males of the indicated genotypes were crossed to virgins of the background

stock for 1–2 generations, before virgins were selected and crossed into the background stock for six further generations. Flies were rebalanced using balancers crossed into the background stock for six generations.

Genetic screen of *Drosophila*

The BDSC deficiency kit was ordered from the Bloomington *Drosophila* Stock Center. Deficiencies covering chromosomes 2, 3, 4 were crossed to flies of the following genotype: w*;;UAS-FUS(R521G), D42-Gal4/TM6BGal80* and reared at 25 ℃. Pharate TM6B-negative pupae were moved to a petri dish and followed for 72 h. The percentage of eclosed flies was defined as ratio of the number of empty pupal cases to the total number of pupal cases.

Eclosion phenotype with modifying lines

Prior to experiments, sgg (31308, 31309, 38293, 35364) and mts (35171, 35172, 41924) RNAi lines were backcrossed to *w + v- w1118* (TRiP lines, marked with vermillion) or *w1118* (VDRC lines, marked with miniwhite) control background for six generations, to ensure that results are not affected by different genetic backgrounds of the flies. 5 sgg or mts RNAi virgins were crossed to 3 *w;;D42-Gal4, UAS-FUS/TM6BGal80* males and females were allowed to lay eggs for 48 h. Parents were removed from the vials and the progeny were allowed to grow at 25 ℃. 14 days after set up, eclosion was scored, counting the number of eclosed versus total TM6B-negative pupae. *w1118* and *w + v-* background strains were crossed in as controls.

Eclosion phenotype with LiCl, OA and LB-100

Lithium chloride (LiCl) (0–15 mM, L9650, Sigma-Aldrich), okadaic acid (OA) (0–50 nM, 459,620, Sigma-Aldrich), or LB-100 (0–100 μM, HY-18597, MCE) was dissolved in milliQ H_2O and added to standard food at the indicated concentrations. For the 0 condition, H_2O alone was added. *w-;;UAS-FUS (WT)* and *w-;;UAS-FUS (R521G)* males were crossed to D42-Gal4 virgins. Females were allowed to lay on drug containing food for 48 h. Crosses were left to develop at 25 °C and eclosion was scored 14 days after set up.

Lifespan

The indicated lines were crossed to *w;Gal80-ts;D42-Gal4, UAS-FUS/TM6B* males on grape agar plates supplemented with yeast paste. Approximately 50 virgins and 20 males were used per cross. Eggs were collected after 24 h into PBS and seeded at a standard density into bottles. Bottles were allowed to develop for 21 days at 18 ℃. Adult male flies (female in the case of sgg null mutant crosses) were briefly anaesthetized on CO_2 and split into vials at a density of ten flies per vial. Approximately 150 flies (15 vials) were analyzed per condition, and exact N numbers are given in supplementary material. Flies were tipped onto fresh food twice a week, and deaths were scored every other day at the beginning and every day toward the end of the experiment. Statistical significance was assessed using log-rank test.

iPSC lines

A previously characterized *FUS* mutant iPSC line from a 17-year-old male ALS patient carrying a de novo mutation (P525L) was used [29, 61]. The FUS-ALS line was compared with its isogenic CRISPR-Cas9 gene-edited isogenic control (P525P) generated by CellSystems (Troisdorf, Germany) [29]. Cells were cultured and differentiated into MNs according to a well-established protocol as described before [29]. The cells were previously collected from the donor with the approval of the ethical committee of the University Hospitals Leuven (S50354).

Immunofluorescence of iPSC-derived sMNs and FUS mislocalization

Drugs (LiCl L9650 Sigma-Aldrich, tideglusib SML0339 Sigma-Aldrich, OA 459620 Sigma-Aldrich, LB-100 HY-18597 MCE) were prepared fresh and dissolved in water (DMSO for tideglusib). Cells were mock treated using an equivalent volume of vehicle. On day 30 of differentiation, cells were briefly washed with PBS, and fixed with 4% paraformaldehyde (PFA) in PBS for 15 min at room temperature. Cells were then washed 3 × 10 min with PBS, followed by a blocking step for 1 h with 5% normal donkey serum (NDS) (D9663, Sigma-Aldrich) in 0.1% PBS-Triton X-100 (PBS-T). Cells were incubated with primary antibodies overnight at 4 ℃ in 2% NDS-PBS-T (Table S5). The following day, cells were washed 3 × 5 min with PBS-T and the secondary antibodies (Table S6) were added in 2% NDS-PBS-T for 1 h at room temperature. Cells were then washed 2 × with PBS and NucBlue™ Live ReadyProbes™ Reagent (Invitrogen) was added at a concentration of 2 drops/mL PBS for 20 min at room temperature to stain the nuclei (Hoechst 33342). Cells were washed 2× with PBS and coverslips were mounted onto slides with ProLong Gold Antifade mounting reagent (P36934, Thermo Fisher Scientific). Cells were imaged with an inverted confocal microscope (SP8 DMi8, Leica Microsystems). Captured images were analyzed using ImageJ software. For nucleocytoplasmic quantification, regions of interest (ROIs) corresponding to the nucleus of the cell and the soma were drawn using the signal in the Hoechst channel before measurements in the FUS channel were taken. A nearby non-cellular ROI was used to determine the average background of each ROI, and these values

were subtracted from the measurements. The ratio of the background subtracted raw integrated densities was used to calculate the nucleocytoplasmic ratio.

NMJ analysis

The same FUS mutant and isogenic control iPSC-derived MNs as described above were used. In addition, human myoblasts were isolated from a biopsy from a 55-year-old healthy woman and cultured as described previously [26, 62]. On day 10, motor neuron neural-progenitor cells (MN-NPCs) were seeded in the two wells and the channel on one side of the microgrooves in the microfluidic device (Xona Microfluidics, XC150) at 125,000 cells per well (250,000 NPCs/device). Similarly, myoblasts were seeded in the two wells and the channel opposite to the MNs in the device at 20,000 cells per well (40,000 myoblasts/device). Myoblasts were differentiated into myotubes and MN-NPCs into sMNs following the established protocol [62]. On day 18, a chemotactic and volumetric gradient was established. MN compartments received 100 µL/well neuronal medium without neurotrophic factor, and myotube compartments received 200 µL/well neuronal medium supplemented with 10 ng/mL BDNF (PeproTech, Rocky Hill, NJ, USA, cat. no. 450-02), GDNF (PeproTech, cat. no. 450-10), and CNTF (PeproTech, cat. no. 450-13) in addition to 20 mg/mL laminin (Sigma-Aldrich, cat. no. L2020-1MG) and 0.01 mg/mL recombinant human Agrin protein (R&D Systems, cat. no. 6624-AG-050). On the same day, both sides of the device were treated with a drug (LiCl 1 mM 48 h, tideglusib 15 µM 48 h, okadaic acid 1 nM 72 h). Mock co-culture devices were kept in parallel without drug treatments. The growth factor and volume gradients, including agrin/laminin, were maintained at each medium change, which was performed every other day for 10 days. On day 28, devices were fixed and stained, and images were taken using an inverted SP8 DMi8 Leica confocal microscope. Quantification of NMJ formation was manual and blinded, based on the neurite/presynaptic marker morphology and/or based on co-localization between presynaptic marker neurofilament heavy chain/synaptophysin with post-synaptic marker α-bungarotoxin in myosin-heavy chain-labeled multinucleated myotubes.

SH-SY5Y cell cultures

SH-SY5Y cells (94030304, Sigma) were cultured in T175 flasks in DMEM:F12 Glutamax medium (ThermoFisher Scientific) supplemented with 10% Fetal Bovine Serum (FBS). Media were changed twice a week. For this, cells were washed with Versene (15040066, ThermoFisher Scientific) and lifted with 0.05% trypsin (25300054, ThermoFisher Scientific). Cells were maintained in an incubator (37 ℃, 5% CO_2). For western blotting, cells were seeded in 6-well plates at a density of 0.15×10^6 cells/mL. 48 h after splitting, fresh media were added containing drug or vehicle. Treatment lasted for 24 h.

SH-SY5Y cell lysis for western blotting

24 h after treatment, cells were washed briefly with PBS. Cells were lysed on ice in RIPA buffer (R0278-500ML, Sigma-Aldrich) supplemented with protease inhibitor (cOmplete™, EDTA-free protease inhibitor cocktail (1836170001, Sigma-Aldrich) and phosphatase inhibitor (Phos-STOP™ 4906837001, Sigma-Aldrich). Cells were scraped and the lysate was pipetted into a pre-chilled Eppendorf tube. Lysis was allowed to proceed for 20 min on ice and cells were centrifuged at 16000×g for 10 min at 4 ℃. Supernatant was transferred into a fresh tube and Pierce BCA Protein assay was performed (23225) according to the manufacturer's instructions. Samples were brought to equal concentrations using addition of RIPA buffer, and Pierce™ Lane Marker Reducing Sample Buffer (39000, Thermo Fisher Scientific) was added to a final concentration of 1×. The samples were boiled for 5 min at 95 ℃.

Motor neuron lysis for western blotting

Cells were briefly washed with DPBS. Cells were scraped in DPBS and transferred to a pre-chilled Eppendorf tube. They were centrifuged for 5 min at 1000×g at 4 ℃. Pellets were then lysed in RIPA buffer (R0278-500ML, Sigma-Aldrich) supplemented with protease inhibitor (cOmplete™ EDTA-free protease inhibitor cocktail, 1836170001, Sigma-Aldrich) and phosphatase inhibitor (Phos-STOP™, 4906837001, Sigma-Aldrich). Lysis was allowed to occur on ice for 30 min. Samples were centrifuged at 14000×g for 10 min at 4 ℃ and the supernatant was collected. Pierce BCA Protein assay (23225) was performed. Samples were brought to equal concentrations, supplemented with Pierce™ Lane Marker Reducing Sample Buffer (39000, Thermo Fisher Scientific), to a final concentration of 1× and boiled for 5 min at 95 ℃.

Drosophila head lysate for western blotting

Five days after induction of expression, adult flies were frozen in liquid nitrogen. Heads were removed by vigorously banging the tube containing frozen flies. Ten fly heads were collected per condition on dry ice and before being homogenized at room temperature in 100 µL of 2× Pierce™ Lane Marker Reducing Sample Buffer (39000) using a power pestle. Samples were boiled in 95 ℃ for 5 min and centrifuged at 20000×g at room temperature for 5 min, and the supernatant was moved to a fresh tube.

Purification of KLC1p antibody

Generation of the rabbit antibody to KLC1 phosphorylated on serine-460 was described before [49]. Prior to use, the antibody was purified using the phospho-peptide (CKVD-SphosPTVTTTLKNL), which was synthesized by Gen-Script, using the High-Affinity Antibody Purification Kit (L00404, GenScript) following the manufacturer's protocol.

Phosphorylation assays in HEK293T cells

HEK293T cells were grown in DMEM/F12 high glucose GlutaMax (Gibco, Waltham, MA, USA, Cat# 31331028) supplemented with 10% standard fetal bovine serum (Gibco, Cat# 10500064) and 2% PenStrep (Invitrogen, Cat# 15140-122) at 37 °C in a humidified atmosphere with 5% CO_2. Cells were free of mycoplasma. HEK293T cells were transfected with FLAG-tagged WT and P525L FUS-encoding plasmids and treated with 10 nM calicheamicin γ1 (MedChemExpress, HY-19609) for 2 h. Next, the cells were treated with 10 nM OA (dissolved in H_2O) for different time periods. Vehicle-treated cells were treated with the same amount of H_2O. Cells were scraped on ice and western blot analysis was performed.

Immunoprecipitation

For immunoprecipitation, HEK293T cells were plated at a density of 2×10^6 cells per dish, 24 h prior to transfection. Cells were transferred using TransIT-Neural Transfection Reagent (Mirus Bio, Madison, WI, USA) according to the manufacturer's instructions in serum-free and antibiotic-free conditions with FLAG-tagged WT FUS. 24 h post-transfection, cells were treated with CLM for 2 h and collected in radio-immunoprecipitation assay buffer (RIPA buffer containing 50 mM Tris, 150 mM NaCl, 0.5% sodium deoxycholate, 0.1% SDS, and 1% NP40) supplemented with protease inhibitors (cOmplete EDTA-free, Roche) and phosphatase inhibitors (Phos-STOP, Cat# 04906837001, Roche). Anti-FLAG M2 affinity gel (Sigma-Aldrich, Cat# A2220) was used to immunoprecipitate FLAG-tagged proteins and the protein complexes were analyzed by western blot.

Western blotting

Western blot was performed using NUPAGE 4–12% Bis–Tris 1.0 mm Mini Protein Gels (ThermoFisher Scientific). The PAGE-ruler prestained protein ladder was used as reference (26616, ThermoFisher Scientific). After electrophoresis (140 V, 400 mA), the gel was transferred to a PVDF membrane (IPVH00010 Immobilon-P transfer membrane, Sigma-Aldrich), using the Mini Trans-Blot Cell system (BIORAD). The membrane was blocked in 5% non-fat dry milk (9999S, Cell Signaling) or 5% BSA (11930, SERVA) diluted in Tris-buffered saline with Tween-20 (TBS-T) for 1 h at room temperature. The membrane was then incubated with primary antibody at 4 °C overnight in 5% BSA in TBS-T. The following day, after washing 3 × 10 min with TBS-T, secondary antibody was added in 5% BSA in TBS-T for 1 h at room temperature. Details of all primary and secondary antibodies are given in Tables S5 and S6. The membrane was then washed 3 × 10 min in TBS-T and developed with the Pierce™ ECL Western Blotting Substrate (Pierce ECL, 32106, Thermo Fisher Scientific) or the SuperSignal™ West Pico PLUS Chemiluminescent Substrate (34580). Images were taken using a chemiluminescence instrument (Image-Quant LAS4000).

Live cell imaging of mitochondrial transport and tracking analysis

To measure mitochondrial neurite transport, iPSC-derived sMNs at differentiation day 30 were incubated with 50 nM MitoTracker™ Green FM (M7514, Invitrogen) in neuronal medium for 20 min at 37 °C. After 20 min, cells were washed and incubated in BrainPhys™ Imaging Optimized Medium (05796, STEMCELL Technologies) for imaging. Images were taken using the Operetta CLS High-Content Analysis System (PerkinElmer) with a 40 × objective at 37 °C and 5% CO_2. The MitoTracker™ Green was excited at ~495 nm and 1-s time-lapse images were taken for 200 s. Video files were analyzed with ImageJ using TrackMate v3.8.0 plugin for total mitochondria quantification and tracking, and time/distance kymographs to quantify the number of moving mitochondria in a selected neurite segment. Moving mitochondria are represented by tilted lines, whereas stationary mitochondria can be discerned as straight vertical lines.

Mouse work

Homozygous mice overexpressing wild-type human FUS ($hFUS^{+/+}$) under the mouse prion protein (Prp) promotor were used in this study (JAX®, stock no. 017916) [45], and wild-type littermates were used as controls. Mice were housed at the KU Leuven animal facility, according to the in-house guidelines, as previously described [8]. At the symptomatic age of 60 days, mice were anaesthetized by intraperitoneal injection of sodium pentobarbital (200 mg/kg) and transcardially perfused with 1 × PBS. Spinal cords were rapidly dissected and snap-frozen in liquid nitrogen. Samples were stored at −80 °C until further use. The animal experiment was approved by the local ethical committee of the KU Leuven (Leuven, Belgium) (P007_2019), and complies with the current laws of Belgium.

Statistics

Data are presented as mean $\pm$ SEM, unless indicated otherwise. Statistical analyses were performed in GraphPad Prism 9.

Results

A genome-wide screen identifies *mts* and *sgg* as candidate modifiers of FUS-ALS in vivo

We performed a genome-wide screen to identify candidate modifiers (suppressors) of FUS toxicity in *Drosophila* (Fig. 1a). We previously showed that motor neuron-specific expression of wild-type or mutant human FUS leads to a severe eclosion phenotype [5]. We therefore generated a recombinant stock of UAS-FUS (R521G) and the D42-Gal4 motor neuron driver line. This stock was maintained over a TM6B-Gal80 balancer, which suppresses expression and is marked with a visible marker. We crossed this screening stock to flies from Bloomington *Drosophila* Stock Center (BDSC) deficiency kit, which consists of a selected set of molecularly defined genomic deletions. We focused on deletions on chromosomes X, 2 and 3, crossing 473 deficiency lines to the screening stock and assessing whether eclosion was rescued. When crossed to a control background, the D42-Gal4 > FUS(R521G) flies were not able to eclose, and therefore, any eclosion could be considered as a rescue. Using this approach, we identified 58 candidate deficiencies that attenuated the mutant FUS pupal lethality.

To identify which genes are mediating the rescue effect of the large deficiencies, we first screened with smaller deletions. In total, we screened 167 smaller deletions and found 24 that modified the pupal lethality. Finally, to identify the actual genes responsible for the modifying effects, we used RNAi lines from the 'VIENNA *Drosophila* Research Center' (VDRC) as well as lines carrying mutations in candidate genes which were likely to result in loss-of-function. We found 18 modifying genes out of 88 extensively tested RNAi lines that attenuated mutant FUS-induced pupal lethality (Table S1). Among these genes were *mts*, the *Drosophila* ortholog of human *PPP2CA,* and *sgg*, the *Drosophila* ortholog of human *GSK3B*.

As a complimentary approach to identify modifying genes, we searched the available literature and found 24 candidate genes which have previously been linked to FUS-associated ALS. Screening this list using RNAi lines and putative null alleles allowed us to identify six more genes involved in FUS-induced neurotoxicity, among them *sgg* (Table S1). As a consequence, we ended up with a total of 24 candidate modifiers, with *mts* being identified through the unbiased approach, and *sgg* through both approaches.

Genetic and pharmacological inhibition of mts and sgg rescue eclosion and lifespan in flies

Our approach yielded a total of 24 genes which modify FUS toxicity when their expression is reduced. To prioritize hits for follow-up, we investigated whether any of these genes fall into a common pathway. mts is the catalytic subunit of the PP2A phosphatase complex in *Drosophila*, while *sgg* is the ortholog of *GSK3B* and has recently been linked to ALS/FTD [58, 60]. PP2A has been proposed to directly reduce GSK3 inhibitory phosphorylation in human cells, and thus acts as an activator of GSK3 [35].

As *mts* and *sgg* were candidate modifiers of FUS-toxicity, we sought to confirm their modifying action in the FUS flies. We first backcrossed several RNAi lines against *sgg* and *mts* into a suitable control genetic background (see Materials and methods) for six generations to avoid genetic background effects. Wild-type (WT) FUS and mutant R521G FUS were expressed in fly MNs using the D42-Gal4 driver along with *mts* or *sgg* RNAi and eclosion was scored. Knockdown of *sgg* led to a rescue of the FUS fly eclosion phenotype for both WT and R521G FUS-expressing flies for all 4 RNAi lines tested (Fig. 1b). Knockdown of *mts* led to a rescue for eclosion in WT and R521G FUS-expressing flies for two out of three of the tested RNAi lines (Fig. 1c), while a third line produced a partial eclosion defect on its own, perhaps explaining its lack of a significant effect (Fig. S1). We next tested the consequence of feeding pharmacological inhibitors to the flies. For this, we used lithium chloride (LiCl), a well-known and widely used GSK3 inhibitor [9, 20], and okadaic acid (OA), a specific inhibitor of PP2A in human cells at concentrations of 1–10 nM [65, 66]. Addition of LiCl to the fly food led to a higher percentage of eclosion for flies expressing FUS in their MNs between a range of doses of 5–15 mM LiCl (Fig. 1d). LiCl only affected eclosion of driver-only (D42-Gal4/+) control flies above 20 mM (Fig. 1d), before becoming developmentally lethal at 100 mM (not shown), suggesting that it is well tolerated by the model. OA similarly rescued the eclosion phenotype of FUS flies, with the best rescue occurring between approximately 10 and 25 nM in fly food (Fig. 1e). Toxicity of OA was only observed above 50 nM (Fig. 1e).

To further validate the modifying ability of *mts* and *sgg*, we tested the effect of their knockdown on the lifespan of FUS-expressing flies. We expressed FUS WT or R521G in adult MNs using the D42-Gal4 driver, but to avoid developmental lethality, we included a temperature sensitive Gal80 allele (Gal80-ts), and allowed the flies to develop at 18˚C where FUS expression was suppressed, before moving adults to 25˚C to induce expression. We have previously shown that expression of either WT or mutant R521G FUS in this manner significantly reduces the lifespan of the flies compared to healthy controls,
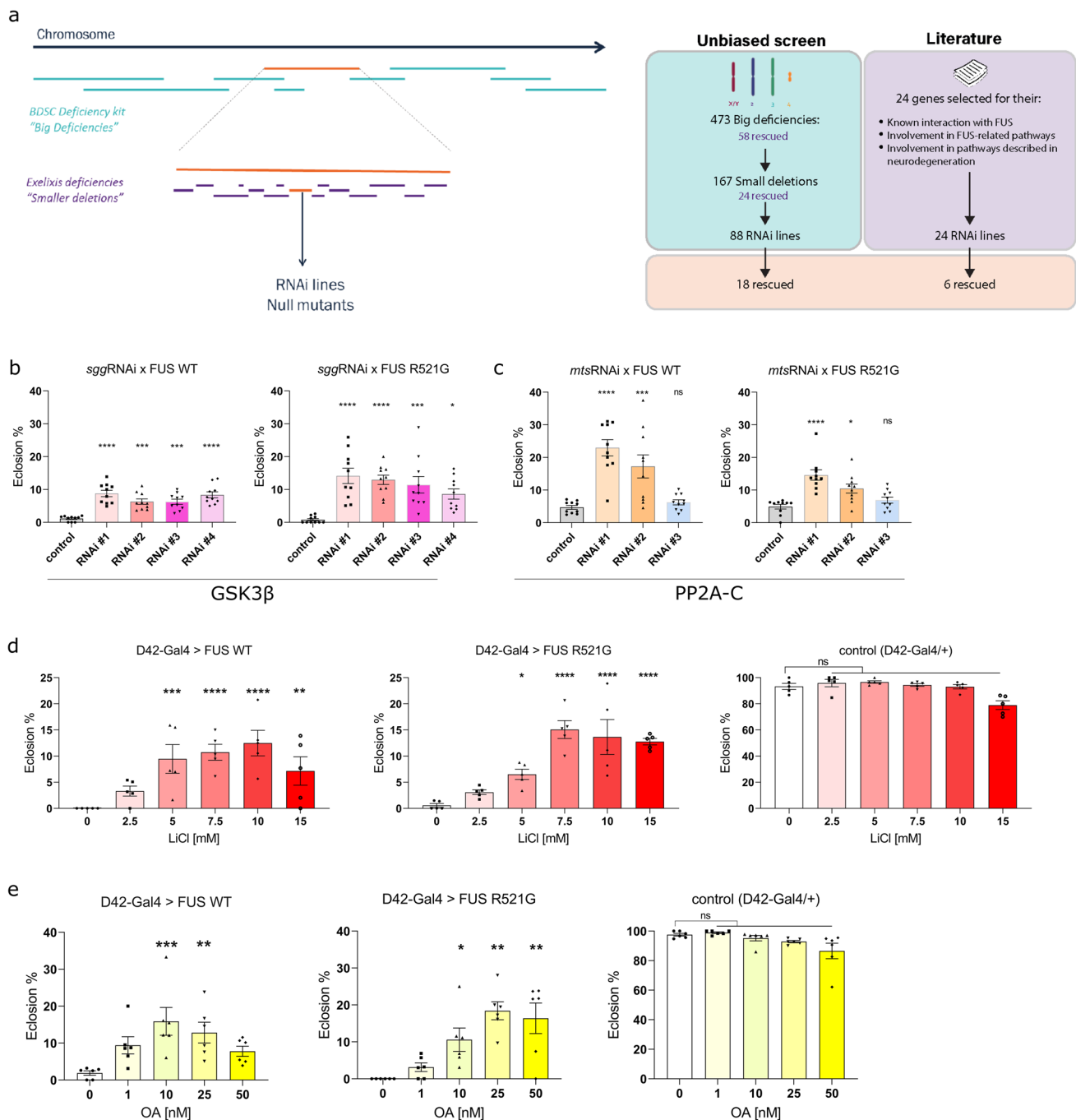
Fig. 1 *mts* and *sgg* are modifiers of FUS toxicity in vivo. **a** Schematic of the experimental set up of the genetic screen in the *Drosophila* FUS model. Candidate genetic modifiers are identified in an unbiased screen, using the BDSC deficiency kit, the Exelixis kit, as well as specific RNAi lines and null mutants against the genes of interest. A complimentary literature-based approach is also used. Eclosion of a fly from the pupal case is categorized as a rescue. In total, 24 genes are identified as candidate modifiers of FUS toxicity. **b** RNAi-mediated genetic knockdown of *sgg* rescues the FUS-induced fly eclosion phenotype. *w + v- w1118* crossed to FUS serves as a control. (*N* = 10 crosses/condition) **c** RNAi-mediated genetic knockdown of *mts* rescues the FUS-induced fly eclosion phenotype. *w1118* crossed to FUS serves as a control. (*N* = 10 crosses/condition). **d** Pharmacological inhibition of sgg by lithium chloride (LiCl) rescues the eclosion phenotype in FUS flies. D42-Gal4/+ serves as a control. (*N* = 5 crosses/condition). **e** Pharmacological inhibition of mts by okadaic acid (OA) rescues the eclosion phenotype in FUS flies. D42-Gal4/+ serves as a control. (*N* = 6 crosses/condition). Values in **b**, **c**, **d**, and **e** are represented as the mean ± SEM. Statistical comparisons between controls and RNAi conditions (**b**, **c**) were determined using one-way ANOVA with Sidak's multiple comparisons test or Kruskal–Wallis test with Dunn's multiple comparisons for each group. Statistical comparisons between controls and treated conditions (**d**, **e**) were determined using one-way ANOVA with Sidak's multiple comparisons or Kruskal–Wallis test with Dunn's multiple comparisons. $^{*}p < 0.05$; $^{**}p < 0.01$; $^{***}p < 0.001$; $^{****}p < 0.0001$, *ns* not significant

leading to death with a median lifespan of approximately 3 weeks [5]. We found that RNAi-mediated knockdown of *mts* or *sgg* led to an extension of the FUS fly lifespan with all of the RNAi lines tested (Fig. 2a, b and Fig. S2).

Importantly, knockdown of *sgg* and *mts* did not alter the levels of FUS protein in the heads of the flies used for lifespan (Fig. 2c, d), suggesting that they exert their effects independently of FUS expression or stability.
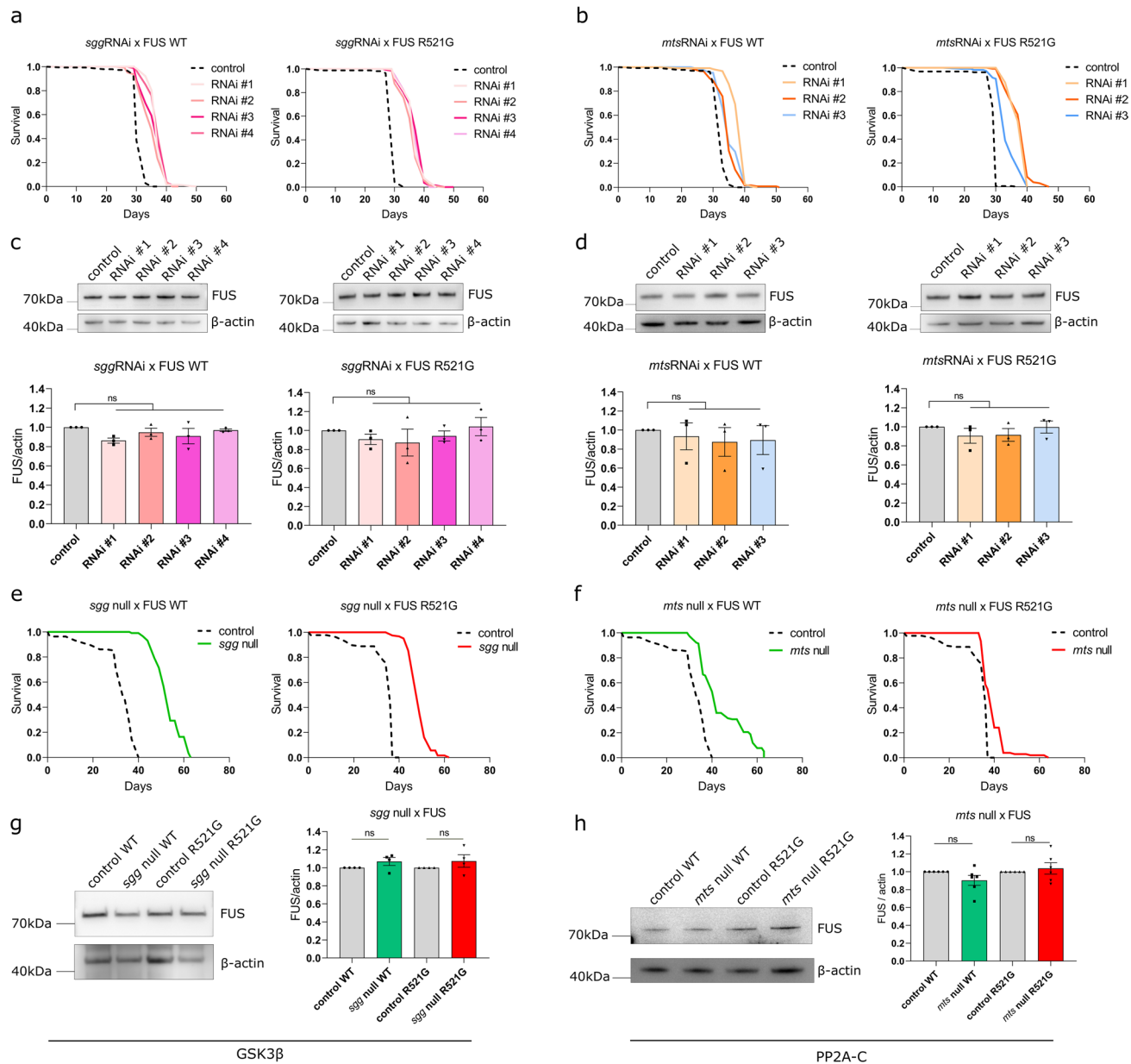

Fig. 2 Inhibition of *sgg* or *mts* extend the lifespan of FUS flies. **a** RNAi-mediated genetic knockdown of *sgg* extends the shortened lifespan of FUS WT and R521G *Drosophila* at 25 ℃. *w + v- w1118* crossed to FUS serves as control (log-rank test, see TableS2 for statistical information). **b** RNAi-mediated genetic knockdown of *mts* extends the shortened lifespan of FUS WT and R521G *Drosophila* at 25 ℃. *w1118* crossed to FUS serves as control (log-rank test, see TableS2 for statistical information). **c, d** Western blotting and quantification demonstrate that FUS expression remains unaltered in *Drosophila* heads after RNAi-mediated knockdown of *sgg* (**c**) or *mts* (**d**) ($N = 3$, mean ± SEM, one-way ANOVA). **e** A heterozygous null

mutation in *sgg* (*sgg^1*) leads to a pronounced extension of the shortened lifespan of FUS WT and R521G flies at 25 ℃. *w1118* crossed to FUS serves as control (log-rank test, see TableS3 for statistical information). **f** A heterozygous null mutation in *mts* (*mts^XE2258*) leads to a pronounced extension of the shortened lifespan of FUS WT and R521G flies at 25 ℃. *w1118* crossed to FUS serves as control (log-rank test, see TableS3 for statistical information). **g, h** Western blotting and quantification show that FUS expression remains unaltered in FUS WT and R521G *Drosophila* heads after heterozygous knock-out of *sgg* (**g**) or *mts* (**h**) ($N = 4$, mean ± SEM, one-way ANOVA). $^{*}p < 0.05$; $^{**}p < 0.01$; $^{***}p < 0.001$; $^{****}p < 0.0001$, *ns* not significant

As an alternative approach to investigate whether reduction of *mts* or *sgg* would lead to a more pronounced extension of the lifespan, we used null mutant lines of the two genes. As homozygous loss-of-function of these genes is developmentally lethal, we introduced a heterozygous loss-of-function. We observed a pronounced lifespan extension after heterozygous loss-of-function of *sgg* and *mts*, confirming the findings using RNAi (Fig. 2e, f). We observed an overall unaltered abundance of FUS protein after *sgg* and *mts* heterozygous knockout (Fig. 2g, h), and we additionally confirmed an approximate 50% reduction of sgg protein levels in the heterozygous mutant flies (Fig. S3). As antibodies against mts are not available, it was not possible to also confirm the level of mts protein in the mts null mutant line.

Altogether, our results show that genetic and pharmacological inhibition of either mts or sgg can rescue FUS-induced developmental neurotoxicity. Moreover, genetic reduction of mts or sgg activity in adult flies can extend lifespan. These two modifying genes appear to act independently of FUS expression. We next sought to determine whether inhibition of the human orthologs of these genes can rescue toxicity in a human cellular model.

Pharmacological inhibition of PP2A and GSK3 rescue hallmark ALS-associated phenotypes in iPSC-derived sMNs

To further confirm the modifying capacity of PP2A and GSK3, we investigated whether their inhibition could rescue hallmark FUS-ALS phenotypes. Cytoplasmic mislocalization of FUS is a pathological hallmark of ALS that has been linked with protein toxicity and neuronal death [17, 36, 73]. Therefore, we decided to investigate whether pharmacological inhibition of PP2A and GSK3 could rescue this phenotype. To assess the modifying effect of PP2A and GSK3 on mislocalization, we used a well-established iPSC line with a de novo point mutation (P525L) in *FUS* from a 17-year-old ALS patient [29, 61]. This patient line was compared with its corresponding CRISPR-Cas9 gene-edited isogenic P525P control [29, 61]. In P525P FUS isogenic controls, FUS was mostly localized in the nucleus (Fig. 3a). In P525L FUS mutant iPSC-derived sMNs, we observed cytoplasmic mislocalization of FUS, which was rescued after a 48 h treatment with 1 mM LiCl (Fig. 3b). Given that LiCl can produce off-target effects [20], we also validated our findings using a highly selective GSK3 inhibitor: tideglusib [38, 42, 53, 55]. Tideglusib (TD) is a non-ATP competitive inhibitor of GSK3, which was well tolerated in phase 2 clinical trials for progressive supranuclear palsy (PSP) [67] and is being investigated in clinical trials for treating GSK3 hyperactivity in Alzheimer's disease [38, 55]. Recently, it has also been suggested as a potential treatment for ALS [42, 58–60]. Excitingly, a 48 h treatment of the P525L FUS sMNs with 15 µM tideglusib also led to a significant rescue of FUS mislocalization (Fig. 3b), confirming that the phenotype alleviation is not due to aspecific effects of LiCl, but thanks to GSK3 inhibition. To inhibit PP2A, we treated the FUS MNs with 1 nM okadaic acid (OA) for 72 h, resulting in a significant rescue of FUS mislocalization (Fig. 3b).

We next determined the effect of pharmacologically inhibiting PP2A and GSK3 on NMJ formation. For this, we used a human-derived co-culture system that is well established in our lab, combining iPSC-derived sMNs and myotubes in microfluidic devices, which allow us to study a functional human NMJ in a compartmentalized system [61, 62]. Mutant FUS-associated NMJ impairment is a phenotype well characterized in this model, as we observe a lower number of NMJs per myotube in the P525L mutant when compared to the P525P isogenic control [61]. On day18 of differentiation, we treated our motor neuron—myotube co-culture system with LiCl (1 mM 48 h), TD (15 µM 48 h), or OA (1 nM 72 h) in both the motor neuron and myotube compartments. On day 28, we fixed the cells and assessed the number of NMJs by performing immunocytochemistry against NMJ markers. Using confocal microscopy, we observed that all three treatments had a positive effect on NMJ formation in the P525L mutant co-cultures, demonstrating the strong modifying capacity of GSK3 and PP2A (Fig. 4 and Fig. S4).

Due to the polarization and length of sMNs, a proper regulation of axonal transport is essential for their function [44]. Defects in axonal transport are considered an early event in ALS pathogenesis, preceding axon retraction and denervation of the muscle [23, 41]. We investigated whether PP2A or GSK3 inhibition could rescue mitochondrial transport deficits in our P525L FUS iPSC-derived sMNs. We performed live cell imaging of mitochondria at day 30 of differentiation. We quantified the total number of mitochondria per 100 µm of neurite, as well as the total number of stationary and moving mitochondria (Fig. S5), allowing us to calculate the percentage of moving mitochondria. Compared to P525P FUS isogenic controls, the percentage of moving mitochondria was significantly lower in P525L sMNs (Fig. 5). After treating the cells with LiCl for 48 h, to inhibit GSK3, tracking analysis showed a clear rescue of mitochondrial transport defects (Fig. 5a, d). Moreover, a similar rescue of mitochondrial transport was observed after treatment with tideglusib (Fig. 5b, e), confirming the modifying capacity of GSK3 inhibition. In addition, OA treatment for 72 h similarly led to a significant improvement of mitochondrial transport (Fig. 5c, f). Although we occasionally observed small differences in the total number of mitochondria per neurite, the drug treatments consistently reduced the number of stationary mitochondria and increased the number of motile mitochondria (Fig. S5).
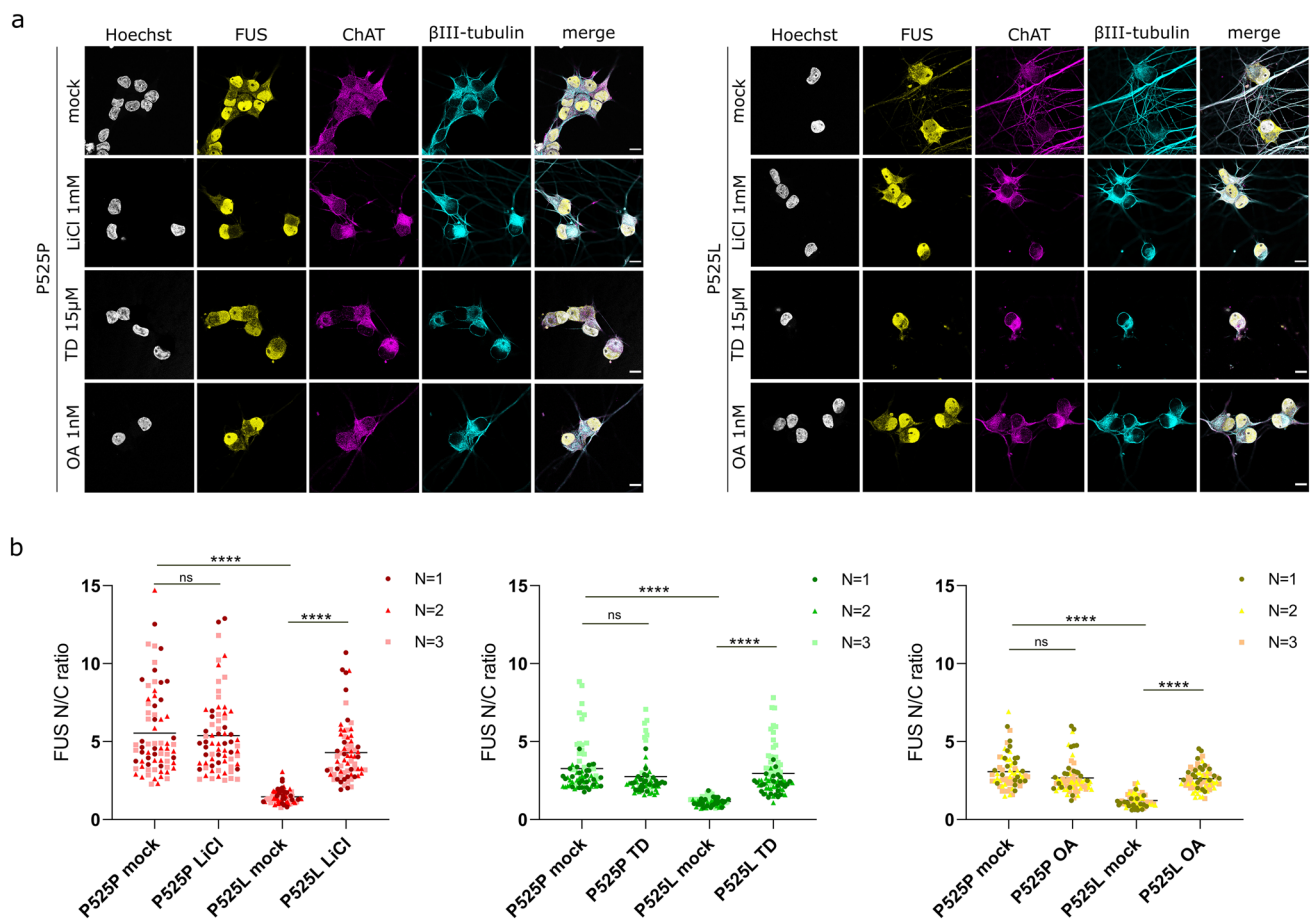
Fig. 3 PP2A and GSK3 pharmacological inhibition rescue FUS cytoplasmic mislocalization in patient iPSC-derived motor neurons. **a**. Representative confocal images showing FUS distribution in patient iPSC-derived motor neurons with the P525L mutation, as well as in P525P isogenic controls after treatment with lithium chloride (LiCl, 1 mM 48 h), tideglusib (TD, 15 μM 48 h) or okadaic acid (OA, 1 nM 72 h). *Scale bars* 10 μm. **b** Quantification of nuclear/cytoplasmic ratios (N/C ratio) fluorescent intensity of FUS in motor neurons shows a rescue of FUS mislocalization after treatments. Each dot represents one analyzed cell. Three different colors indicate data combined from three independent differentiations (70–80 cells/condition). Data are shown as Grand mean; Kruskal–Wallis with Dunn's multiple comparisons test. **** $p < 0.0001$, *ns* not significant

The IC$_{50}$ of OA for PP2A is 0.07–1 nM, which is the range of concentrations that we have used to treat the cells (1 nM). However, OA may also inhibit PP1 in the nanomolar range (IC$_{50}$ 3.4 nM). To confirm our results, we tested a second inhibitor of PP2A, LB-100, a recently developed molecule that is being studied in cancer clinical trials [12, 32], and which is part of a family of compounds with stronger specificity for PP2A compared to PP1 (IC$_{50}$ PP2A = 0.4 μM, IC$_{50}$ PP1 = 80 μM) [39]. Addition of LB-100 to the fly food at concentrations greater than 5 μM rescued the eclosion of the FUS flies and had no apparent toxic effects on healthy controls (Fig. S6). In addition, we tested LB-100 in iPSC-derived sMNs and we observed a significant rescue of mitochondrial movement after treating the cells with 1 μM LB-100 (Fig. S6). Altogether, our results demonstrate that PP2A and GSK3 are modifiers of FUS-induced neurotoxicity both in *Drosophila* and human cellular models.

GSK3 is hyperactive in FUS-ALS due to reduced inhibitory phosphorylation

Recently, reduced GSK3 inhibitory phosphorylation was observed in a FUS mouse model [60], suggesting that GSK3 may become hyperactive in response to a dysfunctional FUS protein. We independently confirmed that reduced GSK3 phosphorylation occurs in the spinal cord of this mouse model at symptomatic stages (Fig. S7). As inhibiting GSK3 was beneficial in our models, we wondered whether this GSK3 hyperactivity was conserved. To determine whether GSK3 is hyperactive in *Drosophila*, we used nSyb-Gal4 combined with Gal80-ts to drive FUS expression pan-neuronally in adult flies for 7 days, and assessed sgg expression and phosphorylation by western blotting (Fig. 6). Consistent with previous reports [81], we observed two major bands of sgg protein in *Drosophila* head lysates corresponding to
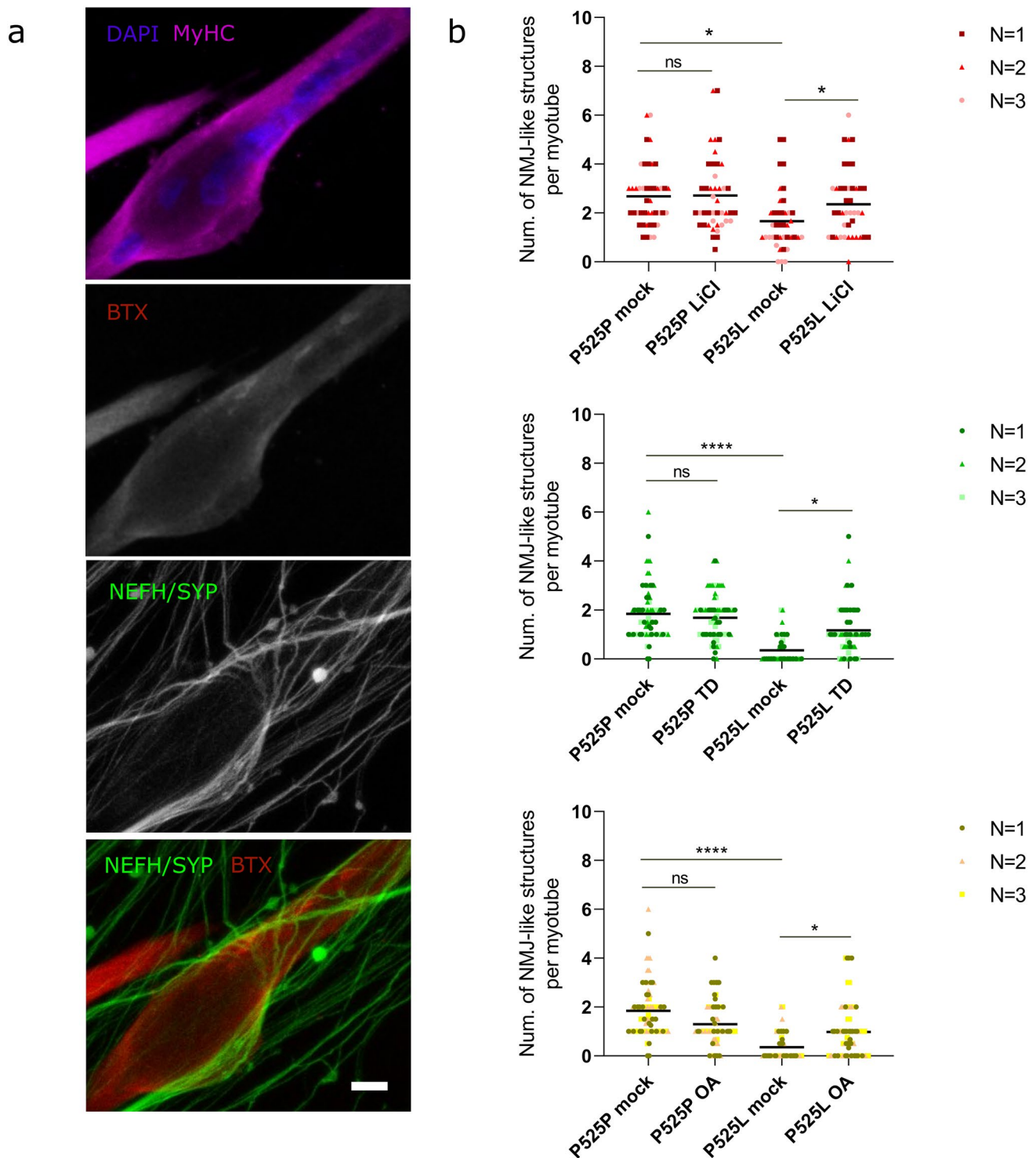
Fig. 4 PP2A and GSK3 inhibition improves ALS-associated NMJ impairments. **a** Representative confocal micrographs of NMJs formed by FUS-P525L cells with LiCl, TD, and OA treatments. NMJs are impaired in FUS-P525L ALS, and inhibition of PP2A or GSK3 improves the phenotype (see Fig. S4 for additional images). *Scale bars* 10 μm. **b** Quantification of NMJ-like structures for all conditions, based on the neurite/presynaptic marker morphology and/or based on Btx (*red*)-SYP/NEFH (*green*) co-localization per myotube. *Each dot* represents one analyzed myotube. *Three different colors* indicate data combined from three independent differentiations (70–80 myotubes/condition). Data are shown as Grand mean; $N = 3$ biological replicates; Kruskal–Wallis test with Dunn's multiple comparisons test. $^*p < 0.05$; $^{****}p < 0.0001$, *ns* not significant
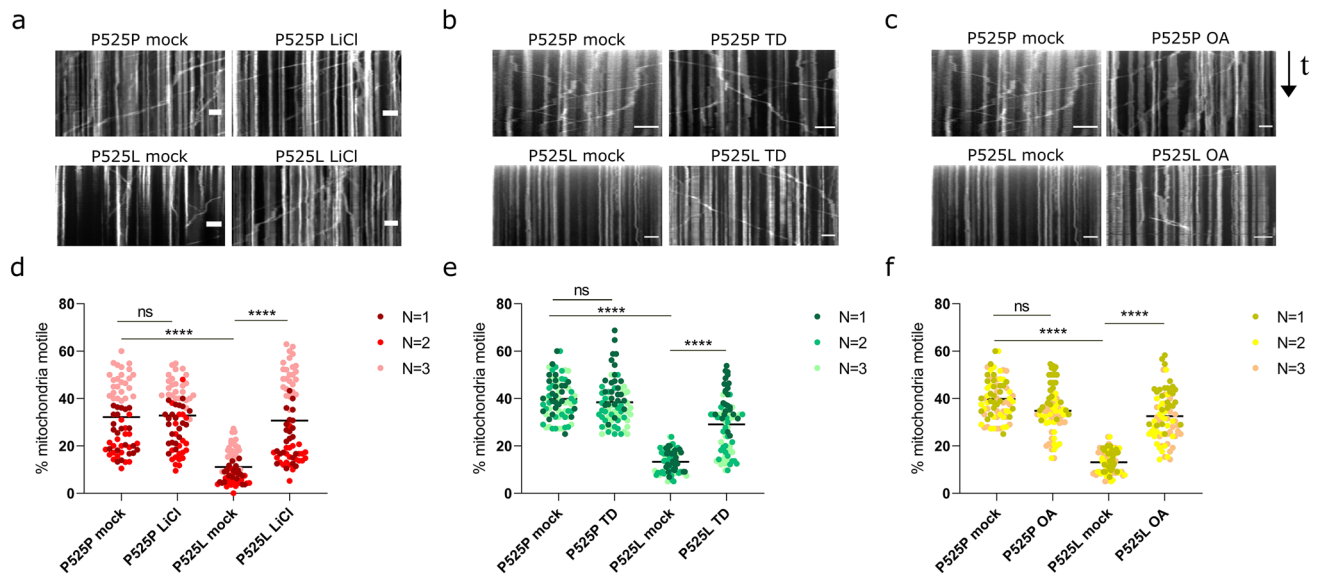
Fig. 5 Pharmacological inhibition of PP2A and GSK3 rescue mitochondrial transport deficits. **a–c** Example kymographs (time-distance plots) of mitochondria (MitoTracker Green) after treatment of 30-day-old P525P isogenic control motor neurons and P525L mutant motor neurons with 1 mM lithium chloride (LiCl) for 48 h (**a**), 15 μM tideglusib (TD) for 48 h (**b**), and 1 nM okadaic acid (OA) for 72 h (**c**). Mock conditions were untreated. *Scale bars* 30 μm **d–f**. Percentage of mitochondria that are motile in the motor neurons (day 30) comparing isogenic control and mutant with or without LiCl (**d**), TD (**e**), and OA (**f**). *Each dot* represents one analyzed neurite. Three different colors indicate data combined from three independent differentiations (70–80 neurites/condition). OA and TD treatments were performed at the same time, so the mock data are the same for both conditions. Data shown as Grand Mean; $N = 3$ differentiations; Kruskal–Wallis with Dunn's multiple comparisons test. $^{****} p < 0.0001$, *ns* not significant
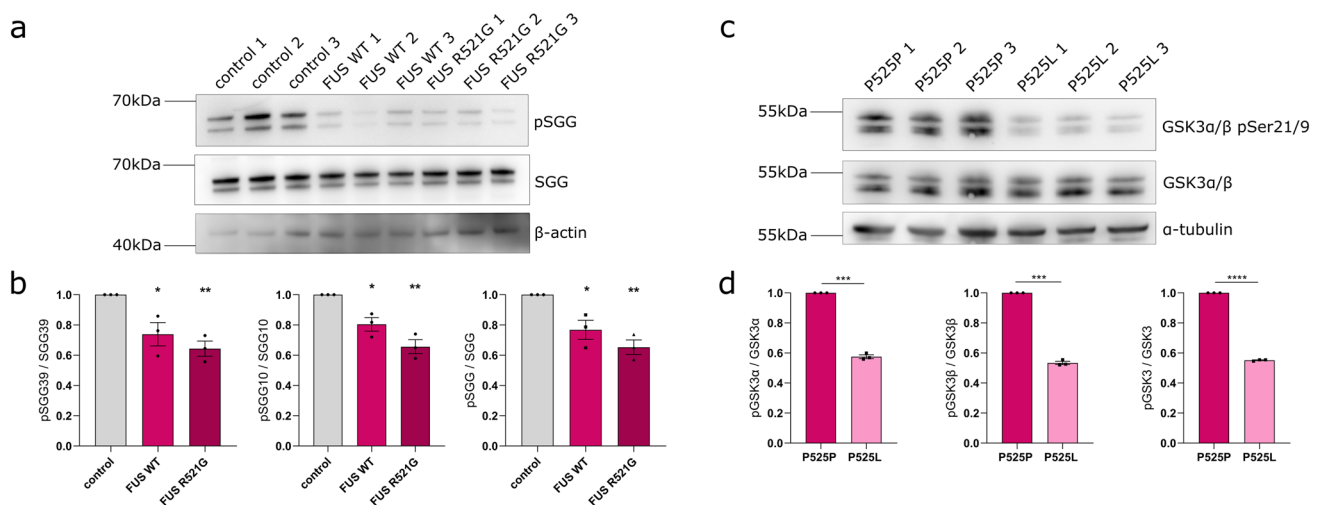
Fig. 6 GSK3 is hyperactive in FUS-ALS due to reduced inhibitory phosphorylation. **a** Western blot showing phospho-sgg and total-sgg protein in control vs FUS WT and R521G flies. Control was *w1118* crossed to Gal80-ts; nSyb-Gal4. In *Drosophila*, the two splice isoforms of GSK3-β, SGG39 (*upper band*) and SGG10 (*lower band*), are seen. Beta-actin serves as a loading control. **b** Quantification of panel a shows that phosphorylation of SGG is reduced in FUS WT and R521G *Drosophila,* for the total-SGG protein and for the individual SGG39 and SGG10 isoforms, while the levels of SGG protein remain unaltered overall ($N = 3$, mean $\pm$ SEM, one-way ANOVA with Sidak's multiple comparisons test). **c** Western blot for GSK3α/β pSer21/9 in iPSC-derived motor neurons from FUS-P525L patients and in their CRISPR-corrected P525P isogenic control. Ser21/9 inhibitory phosphorylation of GSK3α/β appears reduced in FUS P525L patient motor neurons compared to isogenic controls, while the total levels of GSK3α/β remain unaltered among the conditions. The numbers 1, 2, and 3 represent three independent differentiations. Alpha-tubulin serves as a loading control. **d** Quantification of the western blot of panel **c** shows reduced Ser21 and Ser9 inhibitory phosphorylation for GSK3 α and β, respectively ($N = 3$, mean $\pm$ SEM, two-tailed paired t test) $^{*} p < 0.05$; $^{**} p < 0.01$; $^{***} p < 0.001$; $^{****} p < 0.0001$

isoforms SGG10 and SGG39 of the protein. Upon WT and R521G FUS expression, we noticed a significant reduction in the levels of phospho-sgg, while the levels of total-sgg protein remained unaltered (Fig. 6a, b). Therefore, the reduced inhibitory phosphorylation suggests that GSK3 is hyperactive in our FUS flies. To translate our *Drosophila* and mouse findings to human cells, we performed western blotting for phospho-GSK3α/β at residue serine 21/9 in our patient iPSC-derived FUS sMNs on day 30 of differentiation. We found that phospho-GSK3α/β was significantly reduced in mutant P525L FUS sMNs compared to the P525P isogenic controls (Fig. 6c, d), demonstrating that GSK3 inhibitory phosphorylation is also reduced in FUS patient sMNs and suggesting that GSK3 is hyperactive in this model as well.

We wondered whether PP2A may also be affected in FUS-ALS models. Given the availability of a suitable mammalian antibody, we performed western blotting to assess the level of the PP2A catalytic subunit (PP2A-C) in the FUS mouse and patient iPSC-sMNs. Excitingly, we found that the level of PP2A-C was increased in both mouse tissue and in the iPSC-sMNs (Fig. S7c, d and Fig. S8).

PP2A acts upstream of GSK3 affecting its phosphorylation, and GSK3 hyperactivity alone is insufficient to drive toxicity

PP2A has been suggested to modify the phosphorylation of GSK3, affecting its activity [35]. To assess a possible PP2A-GSK3 interaction in our model, we first tested whether PP2A can regulate GSK3 phosphorylation in *Drosophila*. To determine whether mts controls sgg phosphorylation, we overexpressed mts using the pan-neuronal nSyb-Gal4 driver. After aging the progeny for 7 days, we assessed GSK3 phosphorylation using western blotting. We found that *mts* overexpression led to significantly decreased levels of inhibitory phosphorylation of both major sgg isoforms, suggesting that PP2A acts upstream of GSK3 in flies and causes its dephosphorylation (Fig. 7a, b). To determine whether GSK3 hyperactivity is sufficient to lead to neurodegeneration, we overexpressed either wild-type sgg (*UAS-sgg*) or a constitutively active mutant in which the serine 9 phosphorylation site had been replaced with alanine (*UAS-sgg S9 → A*). Overexpression of these sgg variants in fly MNs, using the D42-Gal4 driver, caused an eclosion phenotype, milder than the one observed after FUS expression, suggesting that GSK3 hyperactivity alone can drive toxicity but may not be fully responsible for the strong eclosion defect that we observed in FUS-expressing flies (Fig. 7c). Recapitulating the rescue that we previously saw, addition of LiCl in the food rescued the mild eclosion defect induced by sgg overexpression, increasing eclosion rates from ~60 to ~85% (Fig. 7c). On the contrary, LiCl had no effect on the eclosion of the flies expressing the constitutively active form of sgg, suggesting

that lithium inhibits sgg via increasing its phosphorylation at Serine 9 (Fig. 7c). To determine whether PP2A inhibition could rescue sgg hyperactivity, we added OA to the food of sgg-overexpressing flies. OA significantly increased eclosion of *UAS-sgg* flies, but had no effect on the eclosion of the *UAS-sggS9 → A* flies (Fig. 7d). These data indicate that PP2A and GSK3 act in a common pathway, with PP2A lying upstream of GSK3. Even more importantly, we conclude that PP2A can alter GSK3 inhibitory phosphorylation on this specific Serine9 residue.

These results suggest that in *Drosophila*, one role of PP2A is to modify the activation state of GSK3. To test whether this interaction is conserved in human cells, we treated SH-SY5Y cells with OA, in a concentration range of 0–10 nM. With increasing inhibition of PP2A, we observed increasing levels of phospho-GSK3α/β, indicating that PP2A also controls GSK3 phosphorylation in human cells (Fig. 7e, f).

Increased expression of kinesin-1 is sufficient to rescue FUS toxicity in *Drosophila* models

As we observe defects in the trafficking of mitochondria in iPSC-sMNs, we wanted to assess whether increasing axonal transport in our *Drosophila* model might rescue toxicity. Kinesin-1 is strongly associated with neurodegeneration and ALS [3, 50]. *Drosophila* has a single kinesin-1 heavy chain ortholog (*Khc*) and a single light chain ortholog (*Klc*). Loss of function of *Khc* and *Klc* results in motor dysfunction in *Drosophila* larvae, leading to axonal swellings packed with mitochondria and other fast axonal transport cargo, suggesting that these genes are essential for transport of organelles [27, 33]. Previously, Vagnoni et al. demonstrated that introduction of a genomic rescue construct consisting of a P-element that carries a 7.5 kb genomic fragment including the 3.5 kb kinesin heavy chain transcription unit (P[Khc+]) into wild-type flies can rescue age-related axonal transport deficits [70]. Despite only encoding Khc, this rescue construct has also been reported to increase Klc at the protein level via an unknown mechanism [27].

To rule out genetic background effects, we backcrossed P[Khc+] into the *w1118* control background for six generations and crossed it to the FUS WT and R521G eclosion stock. P[Khc+] rescued the eclosion phenotype of our FUS flies (Fig. 8a).

We also performed lifespan experiments and found that P[Khc+]-carrying FUS flies lived significantly longer than controls (Fig. 8b). Subsequently, we performed western blotting on lysates from heads of flies used in the lifespan experiment and observed that both Khc and Klc levels were significantly increased by the introduction of the P[Khc+] rescue construct (Fig. 8c, d).
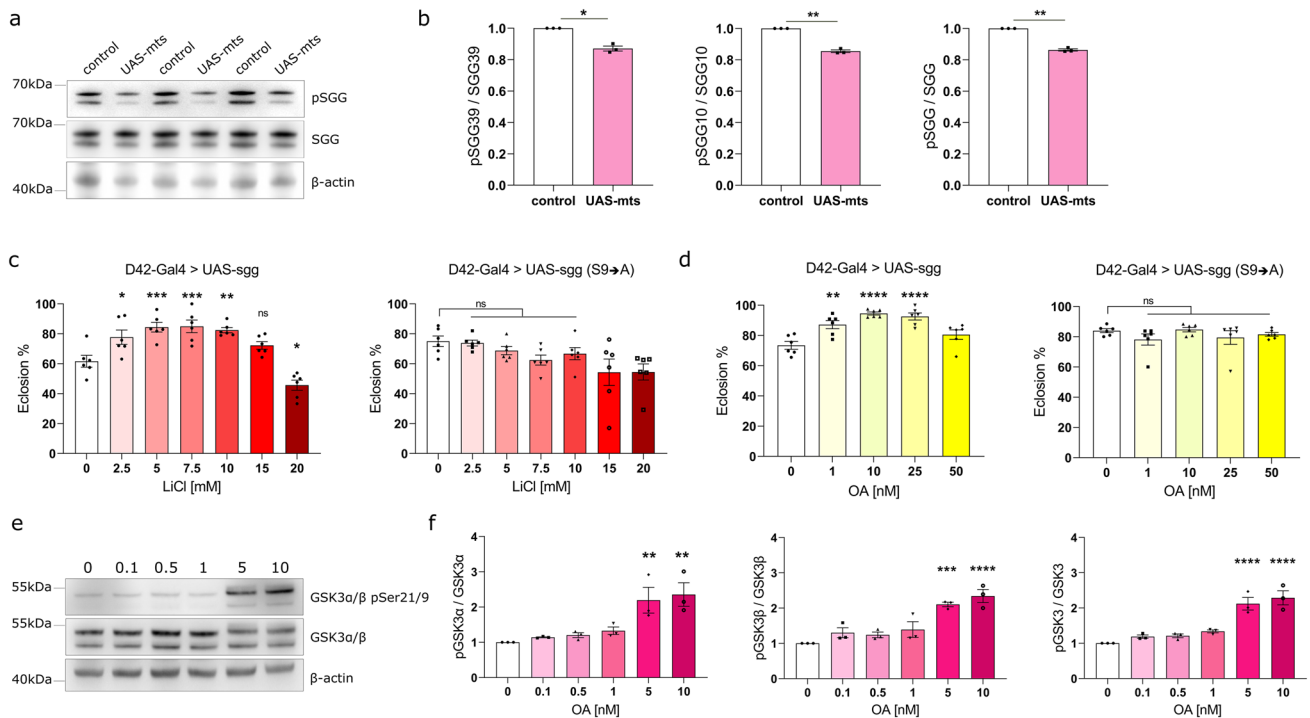
Fig. 7 PP2A acts upstream of GSK3, affecting its inhibitory phosphorylation. **a** Western blot for phospho-sgg and total-sgg protein in control vs. flies overexpressing mts pan-neuronally. Control was *w1118* crossed to Gal80-ts; nSyb-Gal4. In *Drosophila*, the two splice isoforms of GSK3-β, SGG39 (*upper band*) and SGG10 (*lower band*), are seen. Beta-actin serves as loading control. **b** Quantification of panel a shows that phosphorylation of SGG is reduced after mts overexpression in the *Drosophila* brain, for the total-SGG protein and for the individual SGG39 and SGG10 isoforms, while the levels of SGG protein remain unaltered overall ($N = 3$, mean ± SEM, two-tailed paired *t* test). **c** Overexpression of sgg in the fly motor neurons causes a mild eclosion defect, with ~60% flies eclosing. LiCl in the fly food rescues the eclosion deficit to ~85 to 90%. Overexpression of a constitutively active form of sgg (S9 → A) leads to a mild eclosion defect (~75 to 80%) and LiCl has no effect on this deficit. Statistical comparisons between control (0) and treated conditions (2.5–20) were determined using one-way ANOVA with Sidak's multiple com-

parisons ($N = 6$ vials/condition). **d** Overexpression of sgg in the fly motor neurons causes a mild eclosion defect. OA in the fly food rescues the eclosion deficit to ~90 to 95%. Overexpression of a constitutively active form of sgg (S9 → A) also leads to a mild eclosion defect (~80%) and OA has no effect on this deficit. Statistical comparisons between control (0) and treated conditions (1–50) were determined using one-way ANOVA with Sidak's multiple comparisons or Kruskal–Wallis with Dunn's multiple comparisons test ($N = 6$ vials/condition). **e** Western blot for GSK3α/β pSer21/9 in SH-SY5Y cells treated with OA 0–10 nM. Ser21/9 inhibitory phosphorylation of GSK3α/β starts to increase with an increasing dose of OA, while the total levels of GSK3α/β remain generally unaltered. Beta-actin serves as the loading control. **f** Quantification of the western blot of panel e shows a significant increase of Ser21/9 inhibitory phosphorylation for GSK3α/β after treatment with 5 nM OA and 10 nM OA ($N = 3$, mean ± SEM, one-way ANOVA with Sidak's multiple comparisons) *$p < 0.05$; **$p < 0.01$; ***$p < 0.001$; ****$p < 0.0001$, *ns* not significant

Altogether, these results strongly suggest that increasing the levels of kinesin light and heavy chain is beneficial in our fly model.

Kinesin light chain phosphorylation is increased by FUS dysfunction and rescued by inhibition of PP2A/GSK3

Our results showed that inhibition of either GSK3 or PP2A can rescue FUS-induced toxicity in both flies and iPSC-sMNs. FUS is known to be phosphorylated by a number of DNA-damage-associated kinases like ATM [25]. To test whether PP2A could be a phosphatase of FUS, we induced FUS phosphorylation by treating HEK293T cells for 2 h with 10 nM calicheamicin γ1 (CLM), an antibiotic that

cleaves DNA and specifically induces DNA double-strand breaks (DSBs) [16]. We observed robust FUS phosphorylation, visible as an increase in the apparent molecular weight of the protein after SDS-PAGE (Fig. S9a). To test whether PP2A could be affecting the phosphorylation of FUS, we treated the cells with 10 nM OA immediately after the induction of DNA damage and assessed whether OA treatment affected the dephosphorylation of FUS. We failed to observe any significant effect of OA on FUS dephosphorylation after DNA damage (Fig. S9c), suggesting that OA is acting independently of FUS phosphorylation.

To investigate whether a direct physical contact exists between PP2A and FUS, regardless of phosphorylation, we performed pull down experiments. We transfected HEK293T cells with FLAG-tagged WT FUS and treated these with
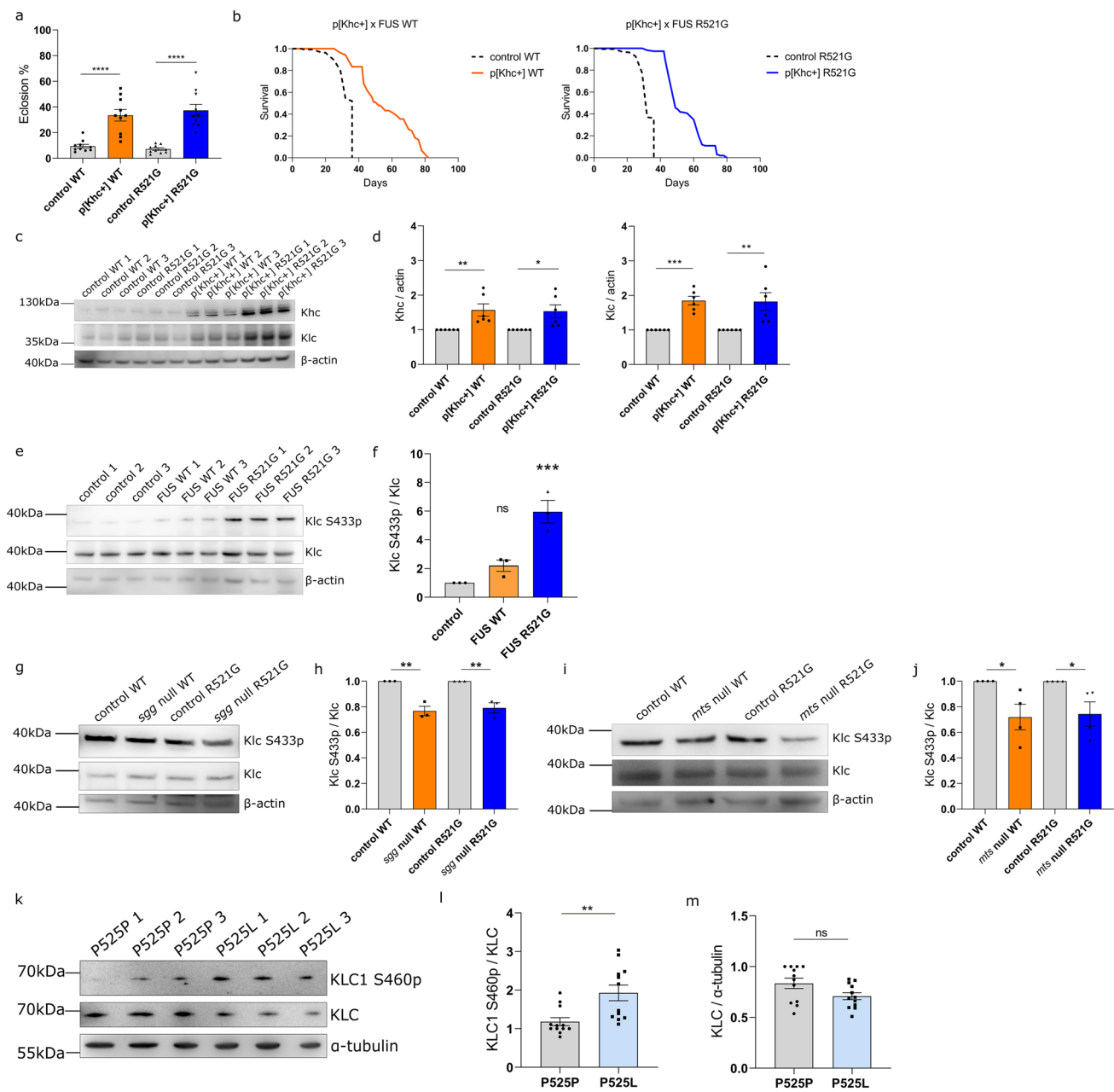
Fig. 8 Kinesin appears dysfunctional in FUS-ALS, perhaps due to hyperphosphorylation by GSK3. **a** Overexpression of Khc using the p[Khc+] stock rescues the FUS-induced fly eclosion phenotype. *w1118* crossed to D42Gal4-driven FUS serves as control. ($N = 10$ crosses/condition). **b** Overexpression of Khc strongly extends the shortened lifespan of FUS WT and R521G *Drosophila* at 25 ℃. *w1118* crossed to FUS serves as control. (see TableS4 for statistical information). **c** Western blot for Khc and Klc in FUS flies vs FUS flies with p[Khc+]. Beta-actin serves as loading control. **d** Quantification of the western blots of panel c show a significant increase in Khc and Klc levels ($N = 6$). **e** Western blot of Klc S433 phosphorylation in control *w1118* VS FUS-expressing flies. **f** Quantification of the western blot of panel e shows increased levels of Klc S433p in FUS flies. **g** Western blot of Klc S433p in FUS flies with *sgg* heterozygous knockout ($N = 3$). **h** Quantification of panel **g** shows that Klc S433p levels decrease after *sgg* inhibition. **i** Western blotting assessing Klc S433p in FUS flies with *mts* heterozygous knockout ($N = 3$). **j** Quantification of panel **i** shows that Klc S433p levels decrease after *mts* inhibition. **k** Western blotting in FUS P525P and P525L MNs, assessing KLC1 S460 phosphorylation. **l** Quantification of panel k reveals increased KLC1 S460p in P525L patient motor neurons compared to isogenic controls ($N = 3$ differentiations). **m** Quantification from panel **k** shows a trend for reduced KLC1 levels in FUS P525L MNs. Values in **a**, **d**, **h**, **j**, and **l** are represented as the mean ± SEM and statistical comparisons were determined using unpaired *t* test. One-way ANOVA with Sidak's multiple comparison test was used for panel **f**. $^*p < 0.05$; $^{**}p < 0.01$; $^{***}p < 0.001$; $^{****}p < 0.0001$, *ns* not significant

10 nM CLM for 2 h. Although the pull down of the FLAG-tagged FUS was efficient, we were not able to detect PP2A on western blot analysis in normal or CLM-treated conditions (Fig. S9b).

These results suggest that the modifying effect of PP2A does not depend on a direct physical interaction with FUS nor on its de-phosphorylating ability, indicating that PP2A acts indirectly to induce FUS toxicity.

Given that PP2A/GSK3 inhibition appears unlikely to affect FUS phosphorylation directly, we wondered whether these proteins could be directly involved in some of the downstream pathologies that FUS induces. Kinesin light chain is a substrate of GSK3 in vivo [6, 46, 78], suggesting that a potential GSK3 hyperactivity in FUS-ALS could lead to kinesin hyperphosphorylation and dysfunction/degradation. Recent studies showed that KLC1 Serine460 phosphorylation causes axonal transport deficits and contributes to neurodegeneration in Alzheimer's disease [49]. Given that this phosphorylation site is well conserved in *Drosophila* (Serine433) [49], we used western blotting to examine Klc S433 phosphorylation in FUS-expressing flies (Fig. 8e). After pan-neuronal expression of either WT or R521G mutant FUS, we observed that Klc S433 phosphorylation levels increased, particularly in R521G-expressing flies (Fig. 8f).

To test the modifying ability of PP2A and GSK3 on this downstream target, we used our *mts* and *sgg* null mutant lines and we examined the levels of Klc S433 phosphorylation after *mts* or *sgg* heterozygous knockout. Excitingly, we saw that the levels of Klc S433 phosphorylation decreased again after *mts* or *sgg* knockdown in both WT and mutant FUS flies (Fig. 8g, h, i, j). These data support our hypothesis that the changes in GSK3 phosphorylation lead to its hyperactivity, increasing kinesin-1 phosphorylation and culminating in dysfunction in FUS-ALS. Last but not least, to translate our *Drosophila* findings of FUS-associated kinesin dysfunction to humans, we performed western blotting in P525P isogenic and P525L mutant FUS iPSC-sMNs. In line with our fly data, we found that KLC1 Serine460 phosphorylation was increased in FUS mutant sMNs (Fig. 8k, l). Moreover, there was a tendency for KLC levels to be reduced in the mutant FUS sMNs on the blot, further indicating a possible dysfunction/degradation of KLC in FUS-ALS (Fig. 8k, m). Altogether, our data show a previously unknown link between GSK3 hyperactivity and kinesin dysfunction, leading to mitochondrial transport deficits in FUS-ALS.

Discussion

The heterogeneity of ALS in terms of its pathology and clinical presentation complicates our understanding of the disease [1, 4, 31, 64]. Since this variability may arise from

the existence of disease-modifying genes, we performed a genome-wide screen in *Drosophila* to discover novel modifiers of FUS-ALS. We identified a total of 24 genes whose loss-of-function rescued the FUS eclosion defect. The genes *mts* (*PPP2CA*) and *sgg* (*GSK3B*) were two of those candidates which we pursued further. Genetic and pharmacological inhibition of mts or sgg rescued FUS-induced phenotypes in *Drosophila*, such as eclosion defects and reduced lifespan. Remarkably, we observed reduced inhibitory phosphorylation of GSK3 and increased abundance of PP2A-C in an FUS-ALS mouse model as well as in mutant FUS iPSC-derived sMNs, suggesting that these proteins are dysfunctional in the disease. Treatment of mutant FUS iPSC-derived sMNs with PP2A or GSK3 inhibitors rescued hallmark ALS phenotypes, such as cytoplasmic mislocalization of FUS, reduced NMJ formation and mitochondrial transport defects, further supporting our finding that PP2A and GSK3 are modifiers of FUS toxicity.

GSK3 is a ubiquitously expressed kinase, whose activity depends on its own inhibitory phosphorylation [13]. The *GSK3B Drosophila* ortholog, *sgg*, is highly conserved (76% amino acid identity compared to GSK3β), and it has been shown that overexpression of human GSK3β can rescue *sgg* loss-of-function associated developmental defects in flies [56]. GSK3 hyperactivity has been linked to neurodegeneration before, mainly to Alzheimer's Disease (AD), and recent studies suggested a possible role of GSK3 in FUS and TDP-43 ALS [58–60]. Notably, loss-of-function of *sgg* has been shown to rescue neuronal dysfunction in a TDP-43 *Drosophila* model [58, 69]. Moreover, our findings are in line with Choi et al., who recently suggested that sgg inhibition could rescue various phenotypes in *Drosophila* overexpressing human FUS [10]. PP2A is a multi-subunit phosphatase highly expressed in the brain, of which PP2A-C (mts) is the catalytic subunit. The *Drosophila* ortholog, *mts*, is also highly conserved, showing 94% amino acid identity to its mammalian counterpart [51]. Recent findings suggest that these two enzymes can affect the activities of each other, with PP2A affecting GSK3 phosphorylation [77]. In our study, we have developed multiple lines of evidence that PP2A affects the level of GSK3 inhibitory phosphorylation. In *Drosophila*, overexpression of the PP2A-C ortholog mts reduced sgg phosphorylation, while okadaic acid, a PP2A inhibitor, rescued sgg overexpression-induced toxicity in a manner dependent on sgg phosphorylation at Serine9. In SHSY-5Y cells, we observed a dose-dependent increase in GSK3α/β phosphorylation in response to PP2A inhibition using OA.

It is currently unclear how FUS alters GSK3 activity in our models. It is interesting to note that the *Drosophila* and mouse models rely on overexpression of human FUS, while the iPSC-sMNs have a mutation in the endogenous FUS gene, suggesting that FUS overexpression has the same

effect as disease-associated missense mutations. Given the fact that we observe the same effect in all systems, our results imply that FUS, or its orthologs in other species, may interact with a conserved factor to induce pathogenesis. We have recently found evidence that nuclear histone deacetylases (HDACs) may become hyperactive in the FUS-ALS mouse model [54]. FUS has been shown to directly interact with HDAC1 [76], a protein which has been shown to upregulate PP2A-C expression when hyperactive in cancer cell lines [11]. Further work will be required to determine whether HDAC inhibition affects PP2A expression in our various model systems, and whether this explains the reduced GSK3 inhibitory phosphorylation that we observed.

Healthy mitochondrial transport is crucial for neuronal survival and homeostasis. Mitochondrial transport deficits are linked with several neurodegenerative disorders, such as Alzheimer's and Huntington's disease [43, 79], hereditary spastic paraplegia [21], Charcot–Marie–Tooth disease [19], as well as ALS with *SOD1, TARDBP,* and *FUS* mutations, and ALS with hexanucleotide repeats in *C9orf72* [22, 24, 30, 47]. Axonal transport is mediated by the motor proteins kinesin and dynein [57]. The kinesin superfamily, mediating anterograde axonal transport, is encoded by 45 mammalian genes, with 38 of them being expressed in the nervous system [30, 57]. We focused on kinesin-1, as the strongest genetic evidence connecting impaired axonal transport with neurodegeneration comes from mutations in the kinesin gene [3, 50]. Kinesin-1 is formed from a dimer of two heavy chains (KHCs), encoded by KIF5A, KIF5B, or KIF5C, which act as the motor domain of the protein, and a dimer of KLCs, which acts as an adaptor for cargoes [27, 30, 57]. KIF5A mutations were recently linked to a number of ALS cases, indicating that alterations in anterograde transport may be involved in the pathogenesis of ALS [7, 50]. Moreover, swellings of organelles and proteins that specifically ensnare kinesin were found in the motor axons of *post-mortem* material from ALS patients [15, 68], and differential expression of kinesin isoforms was observed in the motor cortex of sALS patients [52]. Moreover, it was shown that loss of Klc or Khc function leads to disruption of axonal transport in *Drosophila* and to similar axonal swellings [27].

Various kinases can phosphorylate motor proteins responsible for axonal transport, with previous studies suggesting that GSK3 can modulate kinesin-1-based transport by phosphorylating KLC2 [18, 48]. Inhibiting GSK3 activity in primary cortical neurons of a transgenic mouse model of AD led to restoration of Aβ-induced transport deficits [75]. We found that the reduced neuritic transport of mitochondria in P525L FUS iPSC-derived sMNs can be rescued by pharmacological inhibition of GSK3, either by LiCl or tideglusib. Moreover, PP2A inhibition by OA or LB-100 led to a similar rescue of the phenotype. These data suggest that PP2A and GSK3 could act as modifiers of FUS-induced toxicity

by modulating mitochondrial transport. Khc/Klc overexpression in our FUS flies rescued both eclosion defects as well as the shortened lifespan, suggesting a dysfunction of kinesin-mediated axonal transport in these flies. Using recently generated antibodies against KLC1 Serine460, a phosphorylation site which regulates KLC-cargo binding both in flies and humans [49, 71], we observed that FUS overexpression in *Drosophila* strongly increased Klc phosphorylation. We found a similar hyperphosphorylation of KLC1 in patient iPSC-derived sMNs, suggesting a conservation of this mechanism. Previously, it has been suggested that KLC1 is phosphorylated at Serine460 by ERK in human cells [49]. While the role of GSK3 has not been explored, the fact that *sgg* loss-of-function in *Drosophila* can regulate this event suggests that GSK3 is involved in Serine460 phosphorylation as well. It is somewhat surprising that *mts* loss-of-function reduced Klc phosphorylation in *Drosophila*, given that okadaic acid is thought to increase kinesin-1 phosphorylation via ERK activation in human cells [49]. This difference may be because OA was applied by Mórotz et al. at 50 nM, a dose sufficient to generally inhibit Serine/Threonine protein phosphatases. Our results point toward GSK3 hyperactivity and kinesin-1 dysfunction in FUS-ALS. Since GSK3 can phosphorylate kinesin-1, we conclude that GSK3 can modify axonal transport by acting on kinesin-1. GSK3 hyperactivity is induced after FUS expression, causing extensive kinesin-1 phosphorylation. This may lead to cargo release from the motor protein [48] and may push kinesin into the proteasomal degradation pathway [46], causing axonal transport defects (Fig. 9).

The proposed mechanism above still requires some clarifications. First, while KLC1 Serine460 phosphorylation is sufficient to prevent the interaction with some cargoes, it is currently unclear whether this phosphorylation event would be sufficient to drive the mitochondrial transport defect seen in our sMN cultures. It may be that other residues of KLC1 become hyperphosphorylated in the disease state affecting different aspects of cargo binding, and that S460p is simply a readout of a more global protein-wide hyperphosphorylation event. Further work performing unbiased mass spectrometry in our iPSC-sMNs could be used to explore this further.

Second, while GSK3 hyperactivity has been implicated in multiple FUS-ALS models, we find in flies that overexpression of GSK3 (sgg) or its constitutively active form (S9 → A) is insufficient to fully recapitulate the eclosion defect that we observe in FUS-overexpressing flies. This may suggest that FUS overexpression induces multiple independent pathways leading to toxicity, including, but not limited to, GSK3 hypophosphorylation. Further exploration of other modifying genes identified in our study may shed light on this.

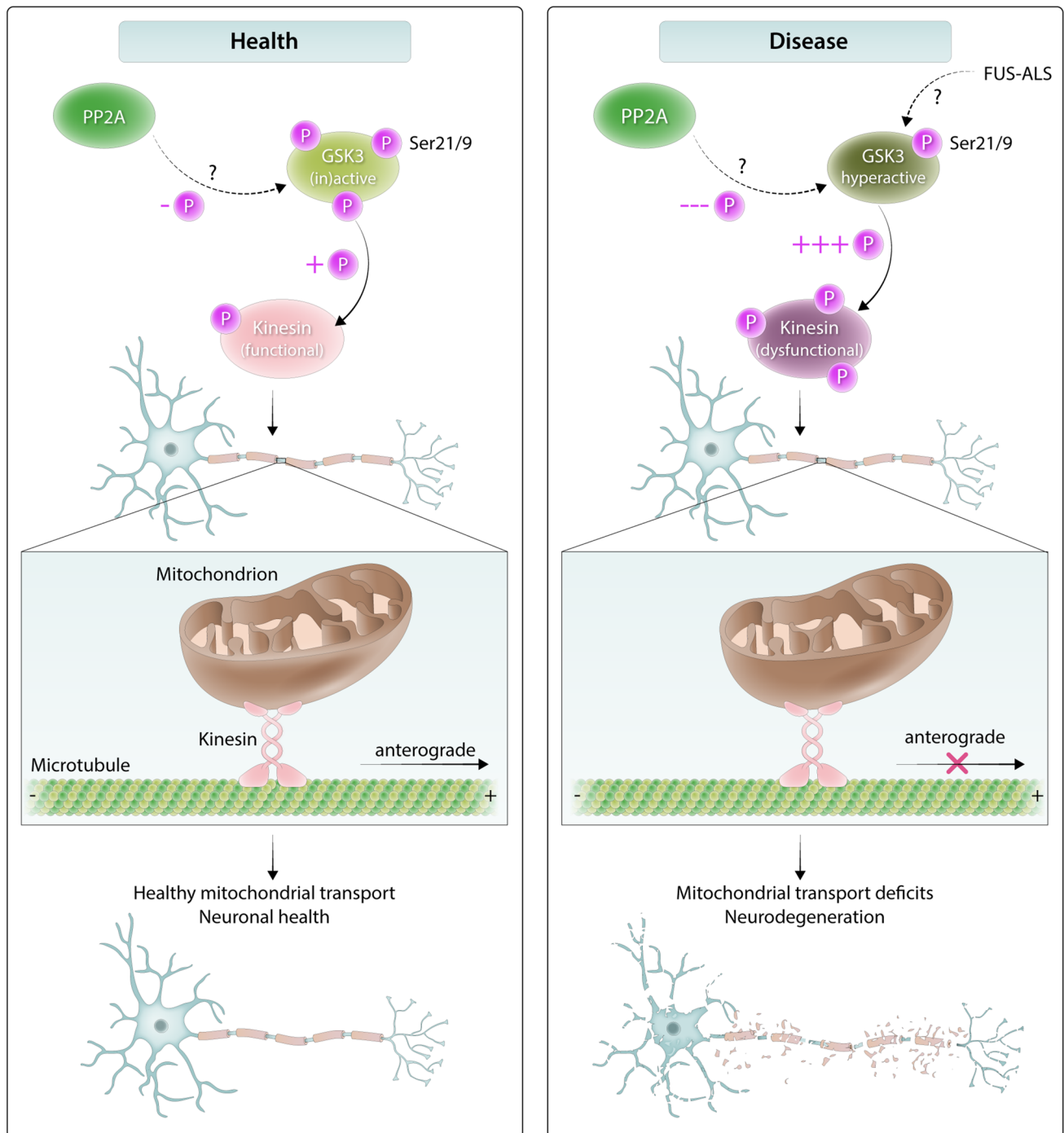We observed that GSK3 and PP2A inhibition was sufficient to return FUS to the nucleus in P525L mutant

Fig. 9 Working model for how GSK3 hyperactivity may be implicated in FUS-ALS. Our current data suggest that in a healthy cell, GSK3 inhibitory phosphorylation is at normal levels, properly regulating kinesin phosphorylation and allowing mediation of mitochondrial transport. However, in FUS-ALS, GSK3 becomes hyperactive, perhaps through the direct or indirect action of PP2A. Subsequently, GSK3 can lead to kinesin hyperphosphorylation and cause cargo release or dysfunction/degradation, leading to mitochondrial transport deficits and neurodegeneration

sMNs. This result may suggest that GSK3 inhibition is not working directly on axonal transport but rather on the localization of FUS itself. However, in contrast to this hypothesis, we and others have observed that removal of the nuclear localization sequence of human FUS is beneficial in flies [5, 34], suggesting that the rescue observed in *Drosophila* is not due to this mechanism. We speculate that the increased nuclear localization of FUS observed in

the treated P525L sMNs may be due to a general increase in health of the cell encouraging nuclear import of FUS. Future experiments which look at the effect of GSK3 and PP2A inhibitors on the localization of fluorescently tagged reporter proteins may help to determine whether these enzymes can affect nuclear import of FUS directly.

In our experiments using human cells, we tested two inhibitors against GSK3 observing consistent results. While LiCl can produce off-target effects [20], tideglusib is GSK3-specific [42]. Similarly, while it is possible that okadaic acid is also affecting PP1, it has a higher specificity for PP2A over PP1 at the concentrations we have used in cells [63]. Nevertheless, to further ensure that specific inhibition of PP2A is responsible for the effects that we observe, we also tested LB-100, a compound which has a strong specificity for PP2A compared to PP1 (IC_{50} PP2A $= 0.4$ μM, IC_{50} PP1 $= 80$ μM) [39], again observing a rescue of disease-relevant phenotypes. Together with the genetic results in flies, and taking into account the concentrations of the inhibitors used in human cells, we suggest that specific PP2A inhibition can rescue disease-relevant phenotypes, although it is worth noting that PP5 may also be targeted by LB-100 [14]. Future experiments inducing a genetic loss-of-function of PP2A-C in the FUS mouse model or in iPSC-sMNs may allow us to confirm this.

Finally, we note that lithium carbonate has already been tested for the treatment of ALS patients, showing no clinical benefit. However, a genetic subgroup analysis indicated that lithium carbonate was beneficial in patients homozygous for the C allele of rs12608932 in UNC13A [72, 80], with a follow-up clinical trial recently announced [80]. Given the apparent heterogeneity in patient response to lithium, further research into its mode of action, and pre-clinical testing of other GSK3 inhibitors like tideglusib is warranted. In the future, it would be interesting to assess whether reduced inhibitory GSK3 phosphorylation is a common feature in ALS patients, and whether the UNC13A genetic status affects this.

Altogether, we tested a hypothesis generated by a high-throughput genetic screen, performing multiple steps of validation. With this work, we showed that PP2A and GSK3 are modifiers of FUS toxicity in *Drosophila* and patient sMNs. Our results are the first to demonstrate that PP2A modifies FUS-mediated toxicity in vivo, and provide a better understanding as to how GSK3 activity may be regulated in ALS. Furthermore, we unraveled a novel mechanistic link between PP2A, GSK3, and kinesin-1, which may lead to mitochondrial transport defects in FUS-ALS (Fig. 9). As a consequence, our study significantly contributes to the understanding of the underlying mechanisms leading to FUS-ALS pathogenesis.

Declarations

Conflict of interest LVDB is head of the Scientific Advisory Board of Augustine Therapeutics (Leuven, Belgium) and is also part of the Investment Advisory Board of Droia Ventures (Meise, Belgium).

References

1. Al-Chalabi A, Tripathi VB (2008) Molecular insights and therapeutic targets in amyotrophic lateral sclerosis. CNS Neurol Disord Drug Targets 7:11–19. https://doi.org/10.2174/187152708783885110

2. Banerjee R, Chakraborty P, Yu MC, Gunawardena S (2021) A stop or go switch: glycogen synthase kinase 3β phosphorylation of the kinesin 1 motor domain at Ser314 halts motility without detaching from microtubules. Development 148:dev199866. https://doi.org/10.1242/dev.199866

3. Baron DM, Fenton AR, Saez-Atienzar S, Giampetruzzi A, Sreeram A, Shankaracharya KPJ et al (2022) ALS-associated KIF5A mutations abolish autoinhibition resulting in a toxic gain of function. Cell Rep 39:110598. https://doi.org/10.1016/j.celrep.2022.110598

4. Beghi E, Mennini T, Bendotti C, Bigini P, Logroscino G, Chio A et al (2007) The heterogeneity of amyotrophic lateral sclerosis: a possible explanation of treatment failure. Curr Med Chem 14:3185–3200. https://doi.org/10.2174/092986707782793862

5. Bogaert E, Boeynaems S, Kato M, Guo L, Caulfield TR, Steyaert J et al (2018) Molecular dissection of FUS points at synergistic effect of low-complexity domains in toxicity. Cell Rep 24:529-537.e4. https://doi.org/10.1016/j.celrep.2018.06.070

6. Brady ST, Morfini GA (2017) Regulation of motor proteins, axonal transport deficits and adult-onset neurodegenerative diseases. Neurobiol Dis 105:273–282. https://doi.org/10.1016/j.nbd.2017.04.010

7. Brenner D, Yilmaz R, Müller K, Grehl T, Petri S, Meyer T et al (2018) Hot-spot KIF5A mutations cause familial ALS. Brain 141:688–697. https://doi.org/10.1093/brain/awx370

8. Burg T, Rossaert E, Moisse M, Van Damme P, Van Den Bosch L (2021) Histone deacetylase inhibition regulates lipid homeostasis in a mouse model of amyotrophic lateral sclerosis. Int J Mol Sci 22:11224. https://doi.org/10.3390/ijms222011224

9. Castillo-Quan JI, Li L, Kinghorn KJ, Ivanov DK, Tain LS, Slack C et al (2016) Lithium promotes longevity through GSK3/NRF2-dependent hormesis. Cell Rep 15:638–650. https://doi.org/10.1016/j.celrep.2016.03.041

10. Choi H-J, Lee JY, Cha SJ, Han YJ, Yoon JH, Kim H-J et al (2022) FUS-induced neurotoxicity is prevented by inhibiting GSK-3β in a Drosophila model of amyotrophic lateral sclerosis. Hum Mol Genet 31:850–862. https://doi.org/10.1093/hmg/ddab290

11. Chuang J-Y, Hung J-J (2011) Overexpression of HDAC1 induces cellular senescence by Sp1/PP2A/pRb pathway. Biochem Biophys Res Commun 407:587–592. https://doi.org/10.1016/j.bbrc.2011.03.068

12. Chung V, Mansfield AS, Braiteh F, Richards D, Durivage H, Ungerleider RS et al (2017) Safety, tolerability, and preliminary activity of LB-100, an inhibitor of protein phosphatase 2A, in patients with relapsed solid tumors: an open-label, dose escalation, first-in-human, phase i trial. Clin Cancer Res 23:3277–3284. https://doi.org/10.1158/1078-0432.CCR-16-2299

13. Cohen P, Frame S (2001) The renaissance of GSK3. Nat Rev Mol Cell Biol 2:769–776. https://doi.org/10.1038/35096075

14. D'Arcy BM, Swingle MR, Papke CM, Abney KA, Bouska ES, Prakash A et al (2019) The antitumor drug LB-100 is a catalytic inhibitor of protein phosphatase 2A (PPP2CA) and 5 (PPP5C) coordinating with the active-site catalytic metals in PPP5C. Mol Cancer Ther 18:556–566. https://doi.org/10.1158/1535-7163.MCT-17-1143

15. De Vos KJ, Hafezparast M (2017) Neurobiology of axonal transport defects in motor neuron diseases: opportunities for translational research? Neurobiol Dis 105:283–299. https://doi.org/10.1016/j.nbd.2017.02.004

16. Deng Q, Holler CJ, Taylor G, Hudson KF, Watkins W, Gearing M et al (2014) FUS is phosphorylated by DNA-PK and accumulates in the cytoplasm after DNA damage. J Neurosci 34:7802–7813. https://doi.org/10.1523/JNEUROSCI.0172-14.2014

17. Dormann D, Rodde R, Edbauer D, Bentmann E, Fischer I, Hruscha A et al (2010) ALS-associated fused in sarcoma (FUS) mutations disrupt Transportin-mediated nuclear import. EMBO J 29:2841–2857. https://doi.org/10.1038/emboj.2010.143

18. Du J, Wei Y, Liu L, Wang Y, Khairova R, Blumenthal R et al (2010) A kinesin signaling complex mediates the ability of GSK-3β to affect mood-associated behaviors. Proc Natl Acad Sci 107:11573–11578. https://doi.org/10.1073/pnas.0913138107

19. d'Ydewalle C, Krishnan J, Chiheb DM, Van Damme P, Irobi J, Kozikowski AP et al (2011) HDAC6 inhibitors reverse axonal loss in a mouse model of mutant HSPB1-induced Charcot-Marie-Tooth disease. Nat Med 17:968–974. https://doi.org/10.1038/nm.2396

20. Eldar-Finkelman H, Martinez A (2011) GSK-3 Inhibitors: preclinical and clinical focus on CNS. Front Mol Neurosci 4:32. https://doi.org/10.3389/fnmol.2011.00032

21. Elert-Dobkowska E, Stepniak I, Krysa W, Rajkiewicz M, Rakowicz M, Sobanska A et al (2015) Molecular spectrum of the SPAST, ATL1 and REEP1 gene mutations associated with the most common hereditary spastic paraplegias in a group of Polish patients. J Neurol Sci 359:35–39. https://doi.org/10.1016/j.jns.2015.10.030

22. Fazal R, Boeynaems S, Swijsen A, De Decker M, Fumagalli L, Moisse M et al (2021) HDAC6 inhibition restores TDP-43 pathology and axonal transport defects in human motor neurons with TARDBP mutations. EMBO J 40:e106177. https://doi.org/10.15252/embj.2020106177

23. Fischer LR, Culver DG, Tennant P, Davis AA, Wang M, Castellano-Sanchez A et al (2004) Amyotrophic lateral sclerosis is a distal axonopathy: evidence in mice and man. Exp Neurol 185:232–240. https://doi.org/10.1016/j.expneurol.2003.10.004

24. Fumagalli L, Young FL, Boeynaems S, De Decker M, Mehta AR, Swijsen A, et al (2021) C9orf72-derived arginine-containing dipeptide repeats associate with axonal transport machinery and impede microtubule-based motility. Sci Adv 7:eabg3013. https://doi.org/10.1126/sciadv.abg3013

25. Gardiner M, Toth R, Vandermoere F, Morrice NA, Rouse J (2008) Identification and characterization of FUS/TLS as a new target of ATM. Biochem J 415:297–307. https://doi.org/10.1042/BJ20081135

26. Gholobova D, Gerard M, Terrie L, Desender L, Shansky J, Vandenburgh H et al (2019) Coculture method to obtain endothelial networks within human tissue-engineered skeletal muscle. Methods Mol Biol Clifton NJ 1889:169–183. https://doi.org/10.1007/978-1-4939-8897-6_10

27. Gindhart JG Jr, Desai CJ, Beushausen S, Zinn K, Goldstein LSB (1998) Kinesin light chains are essential for axonal transport in drosophila. J Cell Biol 141:443–454. https://doi.org/10.1083/jcb.141.2.443

28. Gordon PH (2013) Amyotrophic lateral sclerosis: an update for 2013 clinical features, pathophysiology, management and

therapeutic trials. Aging Dis 4:295–310. https://doi.org/10.14336/AD.2013.0400295

29. Guo W, Naujock M, Fumagalli L, Vandoorne T, Baatsen P, Boon R et al (2017) HDAC6 inhibition reverses axonal transport defects in motor neurons derived from FUS-ALS patients. Nat Commun 8:861. https://doi.org/10.1038/s41467-017-00911-y

30. Guo W, Stoklund Dittlau K, Van Den Bosch L (2020) Axonal transport defects and neurodegeneration: molecular mechanisms and therapeutic implications. Semin Cell Dev Biol 99:133–150. https://doi.org/10.1016/j.semcdb.2019.07.010

31. Hardiman O, Al-Chalabi A, Chio A, Corr EM, Logroscino G, Robberecht W et al (2017) Amyotrophic lateral sclerosis. Nat Rev Dis Primer 3:1–19. https://doi.org/10.1038/nrdp.2017.71

32. Hong CS, Ho W, Zhang C, Yang C, Elder JB, Zhuang Z (2015) LB100, a small molecule inhibitor of PP2A with potent chemo- and radio-sensitizing potential. Cancer Biol Ther 16:821–833. https://doi.org/10.1080/15384047.2015.1040961

33. Hurd DD, Saxton WM (1996) Kinesin mutations cause motor neuron disease phenotypes by disrupting fast axonal transport in drosophila. Genetics 144:1075–1085. https://doi.org/10.1093/genetics/144.3.1075

34. Jäckel S, Summerer AK, Thömmes CM, Pan X, Voigt A, Schulz JB et al (2015) Nuclear import factor transportin and arginine methyltransferase 1 modify FUS neurotoxicity in Drosophila. Neurobiol Dis 74:76–88. https://doi.org/10.1016/j.nbd.2014.11.003

35. Javadpour P, Dargahi L, Ahmadiani A, Ghasemi R (2019) To be or not to be: PP2A as a dual player in CNS functions, its role in neurodegeneration, and its interaction with brain insulin signaling. Cell Mol Life Sci 76:2277–2297. https://doi.org/10.1007/s00018-019-03063-y

36. Kwiatkowski TJ, Bosco DA, LeClerc AL, Tamrazian E, Vanderburg CR, Russ C et al (2009) Mutations in the FUS/TLS gene on chromosome 16 cause familial amyotrophic lateral sclerosis. Science 323:1205–1208. https://doi.org/10.1126/science.1166066

37. Liguori F, Amadio S, Volonté C (2021) Fly for ALS: Drosophila modeling on the route to amyotrophic lateral sclerosis modifiers. Cell Mol Life Sci 78:6143–6160. https://doi.org/10.1007/s00018-021-03905-8

38. Lovestone S, Boada M, Dubois B, Hüll M, Rinne JO, Huppertz H-J et al (2015) A phase II trial of tideglusib in Alzheimer's disease. J Alzheimers Dis 45:75–88. https://doi.org/10.3233/JAD-141959

39. Lu J, Kovach JS, Johnson F, Chiang J, Hodes R, Lonser R et al (2009) Inhibition of serine/threonine phosphatase PP2A enhances cancer chemotherapy by blocking DNA damage induced defense mechanisms. Proc Natl Acad Sci 106:11697–11702. https://doi.org/10.1073/pnas.0905930106

40. Mackenzie IR, Rademakers R, Neumann M (2010) TDP-43 and FUS in amyotrophic lateral sclerosis and frontotemporal dementia. Lancet Neurol 9:995–1007. https://doi.org/10.1016/S1474-4422(10)70195-2

41. Martineau É, Di Polo A, Vande Velde C, Robitaille R (2018) Dynamic neuromuscular remodeling precedes motor-unit loss in a mouse model of ALS. eLife 7:e41973. https://doi.org/10.7554/eLife.41973

42. Martínez-González L, Gonzalo-Consuegra C, Gómez-Almería M, Porras G, de Lago E, Martín-Requero Á et al (2021) Tideglusib, a Non-ATP competitive inhibitor of GSK-3β as a drug candidate for the treatment of amyotrophic lateral sclerosis. Int J Mol Sci 22:8975. https://doi.org/10.3390/ijms22168975

43. McGuire JR, Rong J, Li S-H, Li X-J (2006) Interaction of huntingtin-associated protein-1 with kinesin light chain: implications in intracellular trafficking in neurons. J Biol Chem 281:3552–3559. https://doi.org/10.1074/jbc.M509806200

44. Millecamps S, Julien J-P (2013) Axonal transport deficits and neurodegenerative diseases. Nat Rev Neurosci 14:161–176. https://doi.org/10.1038/nrn3380

45. Mitchell JC, McGoldrick P, Vance C, Hortobagyi T, Sreedharan J, Rogelj B et al (2013) Overexpression of human wild-type FUS causes progressive motor neuron degeneration in an age- and dose-dependent fashion. Acta Neuropathol (Berl) 125:273–288. https://doi.org/10.1007/s00401-012-1043-z

46. Morfini G, Szebenyi G, Elluru R, Ratner N, Brady ST (2002) Glycogen synthase kinase 3 phosphorylates kinesin light chains and negatively regulates kinesin-based motility. EMBO J 21:281–293. https://doi.org/10.1093/emboj/21.3.281

47. Morfini GA, Bosco DA, Brown H, Gatto R, Kaminska A, Song Y et al (2013) Inhibition of fast axonal transport by pathogenic SOD1 involves activation of p38 MAP kinase. PLoS ONE 8:e65235. https://doi.org/10.1371/journal.pone.0065235

48. Mórotz GM, Glennon EB, Gomez-Suaga P, Lau DHW, Robinson ED, Sedlák É et al (2019) LMTK2 binds to kinesin light chains to mediate anterograde axonal transport of cdk5/p35 and LMTK2 levels are reduced in Alzheimer's disease brains. Acta Neuropathol Commun 7:73. https://doi.org/10.1186/s40478-019-0715-5

49. Mórotz GM, Glennon EB, Greig J, Lau DHW, Bhembre N, Mattedi F et al (2019) Kinesin light chain-1 serine-460 phosphorylation is altered in Alzheimer's disease and regulates axonal transport and processing of the amyloid precursor protein. Acta Neuropathol Commun 7:200. https://doi.org/10.1186/s40478-019-0857-5

50. Nicolas A, Kenna KP, Renton AE, Ticozzi N, Faghri F, Chia R et al (2018) Genome-wide analyses identify KIF5A as a novel ALS gene. Neuron 97:1268-1283.e6. https://doi.org/10.1016/j.neuron.2018.02.027

51. Orgad S, Brewis ND, Alphey L, Axton JM, Dudai Y, Cohen PTW (1990) The structure of protein phosphatase 2A is as highly conserved as that of protein phosphatase I. FEBS Lett 275:44–48. https://doi.org/10.1016/0014-5793(90)81435-Q

52. Pantelidou M, Zographos SE, Lederer CW, Kyriakides T, Pfaffl MW, Santama N (2007) Differential expression of molecular motors in the motor cortex of sporadic ALS. Neurobiol Dis 26:577–589. https://doi.org/10.1016/j.nbd.2007.02.005

53. Qu Z, Sun J, Zhang W, Yu J, Zhuang C (2020) Transcription factor NRF2 as a promising therapeutic target for Alzheimer's disease. Free Radic Biol Med 159:87–102. https://doi.org/10.1016/j.freeradbiomed.2020.06.028

54. Rossaert E, Pollari E, Jaspers T, Van Helleputte L, Jarpe M, Van Damme P et al (2019) Restoration of histone acetylation ameliorates disease and metabolic abnormalities in a FUS mouse model. Acta Neuropathol Commun 7:107. https://doi.org/10.1186/s40478-019-0750-2

55. del Ser T, Steinwachs KC, Gertz HJ, Andrés MV, Gómez-Carrillo B, Medina M et al (2013) Treatment of Alzheimer's disease with the GSK-3 inhibitor tideglusib: a pilot study. J Alzheimers Dis 33:205–215. https://doi.org/10.3233/JAD-2012-120805

56. Siegfried E, Chou T-B, Perrimon N (1992) wingless signaling acts through zeste-white 3, the drosophila homolog of glycogen synthase kinase-3, to regulate engrailed and establish cell fate. Cell 71:1167–1179. https://doi.org/10.1016/S0092-8674(05)80065-0

57. Sleigh JN, Rossor AM, Fellows AD, Tosolini AP, Schiavo G (2019) Axonal transport and neurological disease. Nat Rev Neurol 15:691–703. https://doi.org/10.1038/s41582-019-0257-2

58. Sreedharan J, Neukomm LJ, Brown RH, Freeman MR (2015) Age-dependent TDP-43-mediated motor neuron degeneration requires GSK3, hat-trick, and xmas-2. Curr Biol 25:2130–2136. https://doi.org/10.1016/j.cub.2015.06.045

59. Stoica R, De Vos KJ, Paillusson S, Mueller S, Sancho RM, Lau K-F et al (2014) ER–mitochondria associations are regulated by the VAPB–PTPIP51 interaction and are disrupted by ALS/

FTD-associated TDP-43. Nat Commun 5:3996. https://doi.org/10.1038/ncomms4996

60. Stoica R, Paillusson S, Gomez-Suaga P, Mitchell JC, Lau DH, Gray EH et al (2016) ALS/FTD-associated FUS activates GSK-3β to disrupt the VAPB–PTPIP51 interaction and ER–mitochondria associations. EMBO Rep 17:1326–1342. https://doi.org/10.15252/embr.201541726

61. Stoklund Dittlau K, Krasnow EN, Fumagalli L, Vandoorne T, Baatsen P, Kerstens A et al (2021) Human motor units in microfluidic devices are impaired by FUS mutations and improved by HDAC6 inhibition. Stem Cell Rep 16:2213–2227. https://doi.org/10.1016/j.stemcr.2021.03.029

62. Stoklund Dittlau K, Terrie L, Baatsen P, Kerstens A, De Swert L, Janky R et al (2023) FUS-ALS hiPSC-derived astrocytes impair human motor units through both gain-of-toxicity and loss-of-support mechanisms. Mol Neurodegener 18:5. https://doi.org/10.1186/s13024-022-00591-3

63. Swingle M, Ni L, Honkanen RE (2007) Small molecule inhibitors of ser/thr protein phosphatases: specificity, use and common forms of abuse. Methods Mol Biol Clifton NJ 365:23–38. https://doi.org/10.1385/1-59745-267-X:23

64. Swinnen B, Robberecht W (2014) The phenotypic variability of amyotrophic lateral sclerosis. Nat Rev Neurol 10:661–670. https://doi.org/10.1038/nrneurol.2014.184

65. Takai A, Murata M, Torigoe K, Isobe M, Mieskes G, Yasumoto T (1992) Inhibitory effect of okadaic acid derivatives on protein phosphatases. a study on structure-affinity relationship. Biochem J 284:539–544. https://doi.org/10.1042/bj2840539

66. Takai A, Ohno Y, Yasumoto T, Mieskes G (1992) Estimation of the rate constants associated with the inhibitory effect of okadaic acid on type 2A protein phosphatase by time-course analysis. Biochem J 287:101–106. https://doi.org/10.1042/bj2870101

67. Tolosa E, Litvan I, Höglinger GU, Burn D, Lees A, Andrés MV et al (2014) A phase 2 trial of the GSK-3 inhibitor tideglusib in progressive supranuclear palsy. Mov Disord 29:470–478. https://doi.org/10.1002/mds.25824

68. Toyoshima I, Sugawara M, Kato K, Wada C, Hirota K, Hasegawa K et al (1998) Kinesin and cytoplasmic dynein in spinal spheroids with motor neuron disease. J Neurol Sci 159:38–44. https://doi.org/10.1016/S0022-510X(98)00137-3

69. Tziortzouda P, Van Den Bosch L, Hirth F (2021) Triad of TDP43 control in neurodegeneration: autoregulation, localization and aggregation. Nat Rev Neurosci 22:197–208. https://doi.org/10.1038/s41583-021-00431-1

70. Vagnoni A, Bullock SL (2018) A cAMP/PKA/Kinesin-1 axis promotes the axonal transport of mitochondria in aging drosophila neurons. Curr Biol CB 28:1265–1272.e4. https://doi.org/10.1016/j.cub.2018.02.048

71. Vagnoni A, Rodriguez L, Manser C, De Vos KJ, Miller CCJ (2011) Phosphorylation of kinesin light chain 1 at serine 460 modulates binding and trafficking of calsyntenin-1. J Cell Sci 124:1032–1042. https://doi.org/10.1242/jcs.075168

72. Van Eijk RPA, Jones AR, Sproviero W, Shatunov A, Shaw PJ, Leigh PN et al (2017) Meta-analysis of pharmacogenetic interactions in amyotrophic lateral sclerosis clinical trials. Neurology 89:1915–1922. https://doi.org/10.1212/WNL.0000000000004606

73. Vance C, Rogelj B, Hortobágyi T, De Vos KJ, Nishimura AL, Sreedharan J et al (2009) Mutations in FUS, an RNA Processing protein, cause familial amyotrophic lateral sclerosis type 6. Science 323:1208–1211. https://doi.org/10.1126/science.1165942

74. Vandoorne T, Veys K, Guo W, Sicart A, Vints K, Swijsen A et al (2019) Differentiation but not ALS mutations in FUS rewires motor neuron metabolism. Nat Commun 10:4147. https://doi.org/10.1038/s41467-019-12099-4

75. Vossel KA, Xu JC, Fomenko V, Miyamoto T, Suberbielle E, Knox JA et al (2015) Tau reduction prevents Aβ-induced axonal transport deficits by blocking activation of GSK3β. J Cell Biol 209:419–433. https://doi.org/10.1083/jcb.201407065

76. Wang W-Y, Pan L, Su SC, Quinn EJ, Sasaki M, Jimenez JC et al (2013) Interaction of FUS and HDAC1 regulates DNA damage response and repair in neurons. Nat Neurosci 16:1383–1391. https://doi.org/10.1038/nn.3514

77. Wang Y, Yang R, Gu J, Yin X, Jin N, Xie S et al (2015) Cross talk between PI3K-AKT-GSK-3β and PP2A pathways determines tau hyperphosphorylation. Neurobiol Aging 36:188–200. https://doi.org/10.1016/j.neurobiolaging.2014.07.035

78. Weaver C, Leidel C, Szpankowski L, Farley NM, Shubeita GT, Goldstein LSB (2013) Endogenous GSK-3/shaggy regulates bidirectional axonal transport of the amyloid precursor protein. Traffic 14:295–308. https://doi.org/10.1111/tra.12037

79. Weiss KR, Littleton JT (2016) Characterization of axonal transport defects in Drosophila Huntingtin mutants. J Neurogenet 30:212–221. https://doi.org/10.1080/01677063.2016.1202950

80. Willemse SW, Roes KCB, Van Damme P, Hardiman O, Ingre C, Povedano M et al (2022) Lithium carbonate in amyotrophic lateral sclerosis patients homozygous for the C-allele at SNP rs12608932 in UNC13A: protocol for a confirmatory, randomized, group-sequential, event-driven, double-blind, placebo-controlled trial. Trials 23:978. https://doi.org/10.1186/s13063-022-06906-5

81. Wolf FW, Eddison M, Lee S, Cho W, Heberlein U (2007) GSK-3/Shaggy regulates olfactory habituation in Drosophila. Proc Natl Acad Sci USA 104:4653–4657. https://doi.org/10.1073/pnas.0700493104